ZIRAT-6 SPECIAL TOPICS REPORT

AQUARIUS SERVICES CORP.
17 POKAHOE DRIVE
SLEEPY HOLLOW, NY 10591
USA

ADVANCED NUCLEAR TECHNOLOGY
UPPSALA SCIENCE PARK
SE-751 83, UPPSALA
SWEDEN

Mechanical Properties of Zirconium Alloys

Prepared by

R. B. Adamson

Zircaloy Plus

and

Peter Rudling

Advanced Nuclear Technology Sweden AB, Sweden

15 November 2001

Project ANT-P-11-0055

CONTENTS

1. INTRODUCTION

Adequate mechanical properties are crucial for satisfactory fuel assembly performance: 1) in-pile under normal operation, anticipated operational occurrences and accident conditions as well as, 2) under intermediate storage conditions. To ensure that mechanical failure of a fuel assembly does not occur during operation, different fuel design criteria are specified in *Standard Review Plan*, *SRP*. This special topic addresses the mechanical properties related to the fuel design criteria in *SRP* and any other property that is relevant to the performance of the fuel bundle components. Properties addressed include strength and ductility as determined by tests such as tensile, burst, hardness, creep, fracture toughness, and fatigue. It also goes into details of the mechanisms.

The objective of this special topical report has been prepared within the ZIRAT-6 program is to provide members with the basic understanding of the mechanical properties of the fuel components that are crucial for the fuel in-pile performance. The report covers the range from basic information to current knowledge and is written and explained in such a way that even engineers and researchers not familiar with the topic can easily follow the report, find and grasp the appropriate information. This means that the report could be used by the organisation in the training of their internal staff.

The report starts with an introduction, Section 1, and information on the fuel design requirements of the fuel assembly, Section 2. Section 3 reviews some fundamentals and definitions related to the topics covered in this report. Section 4 covers tensile deformation, Section 5 discusses hardness, burst test and Creep deformation, Section 6 deals with fatigue and finally Section 7 focuses on fracture toughness. Section 8 summarizes this report while Section 9 provides the references.

2. FUEL DESIGN REQUIREMENTS

The objectives of the *fuel system*[1] safety review are to provide assurance that

1. The *fuel system* is *not damaged*[2] as a result of normal operation and anticipated operational occurrences,

2. *Fuel system* damage is never so sever as to prevent control rod insertion when it is required,

3. The number of *fuel rod failures*[3] is not underestimated for postulated accidents, and

4. *Coolability*[4] is always maintained

Objective 1. in the above list is formalised in General Design Criterion 10, *GDC 10*, Ref. 1. The interpretation of *GDC10* is done in the Standard Review Plan, *SRP*, Ref. 2. The *fuel system*, nuclear and thermal and hydraulic design are covered in *SRP* sections 4.2, 4.3 and 4.4, respectively. Section 4.2 in *SRP* identifies a number of *fuel system* failure mechanisms that actually have occurred in commercial reactors as well as hypothetical *fuel system* failure mechanisms. For each of these *fuel system* failure mechanisms the *SRP* section 4.2 lists a corresponding design limit that was believed to accomplish objective no. 1 in the above list. These design limits are called Specified Acceptable Fuel Design Limits, *SAFDL*s. It is important to keep in mind that the last time SRP was revised was early in 1980. Thus, the SRP does not include any design limits corresponding to potentially new *fuel system* failure mechanisms related to more recent fuel designs and/or reactor operation strategies.

Fuel rod failures must be accounted for in the dose analysis required by 10CFR Part 100, Ref. 3, for postulated accidents.

---

[1] *Fuel system* consists of assemblies of fuel rods including fuel pellets, insulator pellets, springs, tubular cladding, end closures, hydrogen getters, and fill gas; burnable poison rods including components similar to those in fuel rods; spacer grids and springs; end plates; channel boxes; and reactivity control elements that extend from the coupling interface of the control rod drive mechanism in the core.

[2] *Not damaged* means not only that the fuel integrity is maintained, i.e., no release of radioactivity, but also that the *fuel system* dimensions remain within operational tolerances, and that functional capabilities are not reduced below those assumed in the safety analysis.

[3] *Fuel rod failure* means that the fuel cladding has been breached and radioactivity from the fuel get access to the coolant.

[4] *Coolability* means that the fuel assembly retains its rod-bundle geometry with adequate coolant to permit removal of residual heat even after a severe accident.

The general requirements to maintain control rod insertability and core coolability appear in the General Design Criteria, e.g., *GDC 27* and *GDC 35*. Specific coolability requirements for the loss of coolant accidents, LOCA, are provided in 10 CFR Part 50, Ref. 4.

The *fuel system* design bases must take the four objectives described on the previous page into account. The *SAFDL*s covered in the following does this. In a few cases the *SAFDL*s provide the design limit but in most cases it is up to the fuel vendor to recommend a design limit value, taking a specific failure mechanism into account. The fuel vendor must also provide the background data for the design limits (that are specified by NRC as well as those used by the specific fuel vendor) to ensure that the design limit is relevant. The fuel vendor must also provide data for the specific fuel design that shows that the design limit is met to get their fuel licensed.

The pertinent mechanical tests related to fabrication and in-pile performance issues are summarised in Table 2-1. These mechanical tests will be discussed in detail in the following sections of the report.

In the following section no. 2, however, only the design criteria related to mechanical properties of the zirconium alloy fuel components are discussed. This section is divided into two subsections, one for alloy the fuel components (including the fuel rod) and one for the fuel rod itself.

Table 2-1: Relevant mechanical tests for fabrication and in-pile performance issues

	Fabrication Issues		In-Pile Issues	
Component	**Operation**	**Properties**	**Service Condition**	**Property**
Spacer	Bend Punch Cold roll	UE[5], TE[6] UE, TE UE, FT	Seismic, Handling Vibration Dimensions	IS[7], TE, FT[8] F[9], H[10] IG[11]
Channel	Bend Cold roll	UE, TE UE, TE, FT	Seismic, Handling Vibration Wear	IS TE, FT IS TE, FT F H
Water rod/guide tube	Cold reduce	UE, TE, FT	Handling Assembly support	TE, S[12], IS, FT S, TE, FT
Spacer (grid) spring	Cold roll	TE, UE	Vibration Wear Relaxation	F H IG, C[13]
Tubing	Cold roll	TE, UE, FT	Thermal stress PCI Length, bow Differential pressure	F UW, IGSCC[14], LME[15] IG, C, S S, C, UE, B[16]

[5] Uniform elongation
[6] Total elongation
[7] Impact strength
[8] Fracture toughness
[9] Fatigue
[10] Hardness
[11] Irradiation growth
[12] Strength
[13] Creep
[14] Iodine assisted stress corrosion cracking
[15] Cadmium liquid metal embrittlement
[16] Burst strength

2.1. FUEL SYSTEM DAMAGE

A fuel component is considered as failed according to *SRP* if the component does not comply with the fuel design criteria. Thus, a fuel assembly that exhibits more dimensional changes than the fuel design criterion on dimensional stability specifies, the fuel assembly is considered as failed even though the fuel rods may be intact.

2.1.1. Stress, strain or loading limits

Stress, strain and loads must be limited for spacer grids, guide tubes, fuel rods, control rods, channel boxes and other *fuel system* structural members or otherwise the component may fail. Stress limits that are obtained by methods similar to those given in Section III of the ASME Code, see Section 2.1.1.1.1, Ref. 5 are acceptable. Other proposed limits must be justified.

2.1.1.1.1 Stress limit

Plastic deformation is regarded as material failure according to the ASME Code, and must therefore not occur. *This requirement is fictitious since creep deformation is plastic deformation and creep limited creep strain is allowed.*

Stresses in the *fuel system* structural members may be categorised depending on the origin of the stress and on the geometrical and material discontinuities at the point in the *fuel system* structural member where the stress is calculated.

The ASME Code and comparable design verification systems describe what category of stresses must be taken into account and also how the equivalent stress for each stress category should be evaluated. The design verification systems also specify the maximum allowable equivalent stress in each stress category. The following stress categories, C_i, are defined according to the ASME, Ref. 5, and KTA, Ref. 6, design specifications.

$C_1 = P_m$ = Primary Membrane[17] Stress

$C_2 = P_m + P_b$ = Primary Membrane + Primary Bending[18] Stress

$C_3 = P_m + P_b + Q$ = Primary and Secondary Membrane + Bending Stress

The Japanese Guidebook of Safety Assessment and Review, *JGSAR*, Ref. 7 define the following stress categories

[17] Membrane stress are stresses which have a constant value in the whole material thickness, which means that if the yield stress is exceeded, plastic deformation will occur simultaneously in the whole material thickness.
[18] Bending stresses will result in varying stress levels in the material thickness and when the yield strength is exceeded only local plastic deformation occurs.

C_1 = Primary Stress[19]

C_2 = Secondary Stress[20]

According to the ASME Code, the Tresca formula should be used to calculate the equivalent stress as follows:

$$\sigma_e = \max\left(|\sigma_{11} - \sigma_{22}|, |\sigma_{22} - \sigma_{33}|, |\sigma_{33} - \sigma_{11}|\right)$$

where

σ_{11}, σ_{22}, σ_{33} are the principal stresses, see Section 3.1.

However, according to the KTA and JGSAR Codes of design, the equivalent stress shall be calculated by the von Mises formula, as follows:

$$\sigma_e = \frac{1}{\sqrt{2}}\left[(\sigma_{11} - \sigma_{22})^2 + (\sigma_{22} - \sigma_{33})^2 + (\sigma_{33} - \sigma_{11})^{\frac{1}{2}}\right]$$

For each stress category C_i, let the allowable stress be given by S_i and let *Y(T)* and *U(T)* represent the yield strength and the ultimate strength <u>in unirradiated condition</u>, respectively.

The KTA Code specifies that

$$S_1 = \min(0.90Y(T), 0.5U(T))$$
$$S_2 = \min(1.35Y(T), 0.7U(T))$$
$$S_3 = \min(0.90Y(T), 0.50U(T))$$

and the ASME Code states that

$$S_1 = 1.0S_m$$
$$S_2 = 1.5S_m \text{ where } S_m = \min\left(\frac{Y(T_0)/1.5}{Y(T)/1.5}, \frac{U(T_0)/3}{U(T)/3}\right) \text{ and } T_0 = 20^oC$$
$$S_3 = 3.0S_m$$

[19] Primary stresses are stresses originating from applied loads such as e.g. cladding stresses due to a fuel rod internal overpressure. Primary stresses are not self-limiting and if the yield stress in the component is exceeded, plastic deformation in the whole material thickness will occur. In the case of a fuel rod this would mean that the whole cladding thickness would plastically deform.

[20] Secondary stresses relates to stresses resulting from incompatibility between different volume elements in a component, e.g., caused by a radial temperature gradient in the fuel rod cladding. The secondary stresses are self-limiting, i.e., the stress will relax if the yield strength is exceeded casing the material to locally plastically deform. Exemples of secondary stresses are thermal and bending stresses.

while the JGSAR design specification requires that

$$S_1 = Y(T)$$
$$S_2 = U(T)$$

The design specification then states that the equivalent stress of the combination of the different stresses $\sigma_e^{\max}$ in a given stress category C_i must not exceed the maximum allowable stress S_i for the particular stress category, i.e,

$$\left(\sigma_e^{\max}\right)_{C_i} \le S_i$$

It is important to keep in mind that this stress design criteria is very conservative since material properties in unirradiated condition must be used in the above described calculations. However, the yield strength and the ultimate strength material values are dramatically increased during irradiation the first couple of months of the unirradiated material, thus increasing the margin towards maximum allowable stress.

This stress design criteria is the reason for selecting a higher strength fuel cladding material for PWRs compared to BWRs. The fuel cladding stresses are much higher in the former case due to a larger system-rod differential pressure. Therefore, Stress Relieved Cladding, SRA, Zry-4 or Zry-2 with a much higher strength was needed historically in PWRs while a softer, Recristallised, RXA, material could be used for BWRs. Since Nb additions to Zirconium have a significant solution hardening effect, materials such as M5, Zr1Nb, can be used in PWRs in RXA state.

2.1.1.2.1 Strain limit

At stresses below the yield strength, the material may deform during irradiation due to creep deformation. The *SRA* does not however specify a specific creep strain limit.

For BWR fuel rods a maximum allowable equivalent plastic strain of 2.5 % are sometimes used by fuel vendors corresponding to about 1.5 % plastic tangential strain. The initial creep down, due to larger system than rod internal pressure, of the fuel cladding onto the fuel pellet is not taken into account. Only the outward creep strain after pellet/cladding contact has occurred is limited. This outward creep is due to pellet swelling during irradiation.

For PWRs a maximum allowable creep strain corresponding to a 1 % increase in fuel rod diameter compared to the initial diameter is sometimes used. This limit is related to the risk of getting *departure* from *nucleate boiling*, *dnb*, if the diameter increase becomes too large to enable the coolant to effectively cool the fuel rod.

In-reactor creep tests have shown that the creep ductility, i.e., the amount of creep strain to failure, is much larger than the values provided in this section.

2.1.2. Fatigue limit

Fatigue stresses may be induced in the fuel assembly components due to, e.g., the turbulent coolant flow.

According to the *SRP*, the cumulative number of strain fatigue cycles on the structural components mentioned in section 2.1.1 should be significantly less than the design fatigue lifetime, which is based upon the data by O'Donnel and Langer, Ref. 8, and includes a safety factor of 2 on stress amplitude or a safety factor of 20 on the number of cycles. Other proposed limits may be used but must be justified according to the *SRP*.

In design calculations the fuel vendor must show that alternating bending stresses due to dynamic loads must be below ± 50 MPa.

Normally the dynamic stress is much below ± 50 MPa in the structural components and therefore there is a lot of safety margin regarding fatigue failures.

2.1.3. Fretting wear

According to the *SRP f*retting wear at contact points on the structural components mentioned in section 2.1.1 should be limits. The allowable fretting wear should be stated in the Safety Analysis Report and the stress and fatigue limits in sections 2.1.1 and 2.1.2 should presume the existence of wear.

2.1.4. Oxidation, Hydriding, and CRUD buildup

Oxidation, Hydriding and CRUD buildup should be limited according to the *SRP*. The allowable oxidation, hydriding and CRUD levels should be discussed in the Safety Analysis Report and should be shown to be acceptable. These levels should be presumed to exist when the stress calculation is done in sections 2.1.1 and 2.1.2.

Today *NRC* are using a maximum oxide thickness value of 100 microns for PWRs. This value is calculated as the average value of oxide thickness along the cladding circumference at a specific elevation for the fuel rods. The limit of the oxide thickness is related to that a larger than the maximum allowable thickness would impose such a large obstacle to the surface heat flux, due to the lower thermal conductivity of the oxide compared to the metal, that an increase in the oxide thickness would increase the cladding temperature. This temperature increase would then increase the corrosion rate and an even thicker oxide would form that in turn would increase the cladding temperature further. Thus, a thermal feedback effect would result that would result in mechanical failure of the cladding since higher temperature lowers the material yield strength.

The reason for limiting the hydrogen content is that zirconium hydride, that is brittle, may form at hydrogen contents larger than the solubility limit that is about 100 wtppm at operating temperature. *NRC* has not specified any maximum allowable hydrogen content but some fuel vendors are using a design limits in the range of 500 to 600 wtppm. Again these are average values and consequently much higher local values can exist while still meeting the vendor design criterion.

2.1.5. Dimensional stability

Dimensional changes such as rod bowing or irradiation growth of fuel rods, control rods, and guide tubes should be limited according to the *SRP*. This means that, e.g., fuel rod elongation due to irradiation creep and growth, hydriding and *PCMI* (fuel rods only) must be taken into account in the fuel design to ensure that large enough gaps exists between:

- the top end plugs and top tie plate
- the bottom end plugs and bottom tie plate

If the above mentioned design gaps are too small, the fuel rod will get in contact with the tie plates and further rod elongation will result in fuel rod bowing, that in turn may lead to dry-out and/or rod-rod fretting failures (if neighbouring rods get in contact with each other).

According to the *SRP* the insertability of the control rods must be ensured. This requirement is fulfilled by ensuring that the vertical lift-off forces must not unseat the lower tieplate from the fuel support piece such that the lateral displacement of the fuel assembly occurs. In a PWR this is accomplished by ensuring that the net holding down force from gravitation and holding down springs and is larger than the corresponding sum of lifting forces due to buoyancy and the upward coolant flow. However, if the net holding down force becomes much larger than the net lifting force, fuel assembly elastic[21] bowing may occur. Lower creep strength of the guide tubes will result in larger tendency to transform the elastic bowing stresses into plastic strain, i.e., the fuel assembly keep its bowed configuration upon unloading. During reloading of the core such bowed fuel assemblies will also result in bowing of adjacent fresh straight fuel assemblies. If the fuel assembly bowing becomes large enough, complete control rod insertion may not be accomplished due to too large frictional forces between the control rod and the guide tube inner surfaces. Excessive elongation of the guide tubes due to irradiation growth and/or hydriding may result in a larger fuel assembly bowing tendency if this has not been accounted for in the fuel design. In BWRs, excessive fuel channel bowing may result in control rod insertion difficulties.

Other issues that may result from excessive fuel assembly/channel bowing are decreased thermal margins (*dnbr/CPR* and *LOCA*).

The dimensional changes must also be limited to allow fuel assembly handling during outage.

[21] Elastic bowing means that the fuel assembly will retain its original straight shape upon unloading.

2.1.6. Rod internal pressure

According to *SRP*, the fuel and burnable poison rod internal pressures should remain below the nominal reactor system pressure during normal operation unless otherwise justified. Today, must regulatory bodies including *NRC,* accept some limited rod internal overpressure.

If the rod internal pressure becomes larger than the reactor system pressure, the fuel cladding may start to creep outwards. If the fuel cladding outward creep rate becomes larger than the fuel swelling rate (due to fission product production during irradiation), the pellet-cladding gap may increase. This phenomenon is named liftoff. Since this gap constitute a significant barrier towards the heat flux, an increased gap may result in an increase in fuel pellet temperature. This higher temperature will in turn increase the fission product release rate thus increasing the fuel rod overpressure even more leading to an even higher outward cladding creep rate. Thus, a thermal feedback effect may result that could quickly lead to *fuel failure*. A larger clad creep strength would allow higher rod internal overpressures before liftoff will occur.

The rod internal pressure will also have a significant impact on

- fuel rod ballooning tendency during a *LOCA* and,
- fuel rod outward creep during intermediate storage. To ensure that creep fracture does not occur, a maximum allowable creep strain must be assessed. In US a maximum of 1 % creep strain has been proposec.

2.2. FUEL ROD FAILURE

SRP states that to meet the requirements of

- *GDC10* as it relates to *SAFDL*s for normal operation and anticipated operational occurrences and,
- 10CFR Part 100 as it relates to fission product release for postulated accidents,

fuel rod design criteria should be given for all known *fuel rod failure*[22] mechanisms. Different *fuel rod failure* mechanisms that are related to mechanical properties of the claddings are discussed in the following. As was the case for the fuel systems, it is mostly up to the fuel vendor to define a criterion for each fuel rod failure mechanism listed in the *SRP* to ensure that this failure mechanism will not occur during normal operation and anticipated operational occurrences. However, in some cases *SRP* provides with the fuel rod design criterion.

[22] Fuel rod failure occurs when the fuel cladding has lost its integrity and radioactive fission products may be released to the coolant.

2.2.1. Cladding collapse

Due to the larger system compared to the rod internal pressure, the fuel cladding will be subjected to compressive stresses. If these stresses become large enough, the cladding tube may either momentarily buckle elastically or if the stresses exceeds the yield strength, may result in collapse due to plastic deformation. To prevent elastic buckling and plastic deformation, the fuel vendor has to show by calculations that the fuel cladding stresses are below those resulting in elastic buckling or plastic deformation.

It is obvious that a prerequisite for this fuel rod failure mechanism to occur is that an axial gap exists in the fuel pellet column. This situation is unlikely to occur today with the good fuel manufacturing techniques and control methods that are used by the fuel vendors. Still, the fuel vendor has to assume that a fuel pellet column gap exists, e.g., due to pellet densification, and the vendor must show that the fuel cladding will not collapse, either elastically or plastically. According to *SRP* , a collapsed cladding has to be regarded as a *failed fuel rod* due to the large strains that are accompanying this collapse process.

2.2.2. Excessive Fuel Enthalpy[23]

The *SRP* states that for a severe reactivity initiated accident, *RIA*, in a BWR at zero or low power, fuel rod failure is assumed to occur if the radially averaged fuel rod enthalpy is greater than 170 cal/g at any axial elevation. For full power *RIA*s in a BWR and all *RIA*s in a PWR, the thermal margin criteria, *DNBR* and *CPR*, are used as fuel rod failure criteria to meet the guidelines of the Regulatory Guide 1.77, Ref. 9. The energy deposition in the fuel during a *RIA* transient will result in a thermal expansion of the fuel pellet that may result in fuel cladding tensile stresses/strains, provided that the pellet-cladding gap prior to the *RIA* transient is small enough. If the fuel cladding stresses/strains becomes large enough, the fuel cladding may fail due to *PCMI*[24] or *PCI*[25].

The value of 170 cal/g is however based upon test results of unirradiated and irradiated fuel with low burnups. *RIA* tests in puls reactor over the last decade have shown that lower energy depositions than 170 cal/g may result in *fuel rod failures* for high burnup fuel. This lower energy deposition leading to failures seems to be related to the embrittelement effects of (a) hydrides in the claddings and, (b) the oxide thickness at the fuel cladding outer surface (a crack formed in the brittle oxide during the *RIA* transient may propagate into the fuel cladding). Both the oxide scale formed on the fuel cladding outer surface and the cladding hydrides are a result of the cladding oxidation during irradiation. Thus, a clad strain limit would ensure clad integrity during a RIA event.

---

[23] During a reactivity transient, additional energy will be deposited in the fuel pellet. The enthalpy is a measure of how much energy is deposited during such a transient.

[24] *Pellet Cladding Mechanical Interaction* failure results due to plastic deformation, without iodine, larger than the cladding ductility.

[25] *Pellet Cladding Interaction* failure results due to iodine assisted stress corrosion cracking.

2.2.3. Pellet/Cladding Interaction, *PCI*

According to the *SRP*, there is no current criterion for fuel failure resulting from *PCI*. Two related criteria should be applied, but they are not sufficient to preclude *PCI* failures.

- The transient induced uniform elastic and plastic strain should not exceed 1%. Since *PCI* failures may occur at lower strains than 1 %, this criterion is not sufficient to ensure the non-occurrence of *PCI* failures. It is interesting to note that not even the R&D branch of NRC, Ref. 10, recalls today the basis for this 1 % criterion.

- Fuel pellet melting should be avoided.

3. BASICS

3.1. DEFORMATION

Before discussing mechanical properties as revealed by various testing techniques, it is instructive to review some fundamentals and definitions. Important assumptions usually made are that a component or metal specimen is continuous, homogeneous and isotopic. That is, the component material does not contain voids or empty spaces, its properties are the same at all locations, and it's properties do not vary with direction or orientation. While the first two are generally true (on a macroscopic or large scale) for zirconium alloys, the last (isotropy) is not. Except when the component is quenched rapidly from a high temperature (as in welding or for a particular heat treatment involving quenching from the beta phase, >960°C (1233 K)) zirconium alloy properties of all kinds vary significantly in different directions. But for the current discussion, we will assume isotropy. A few definitions will be useful.

The cylindrical bar in Figure 3-1 with an initial gage length, L_o, is subjected to an axial tensile load, P. The external load, P, is balanced by an internal resisting force

$$P = \int \sigma da$$

where σ is the stress normal to the end plane of the cylinder. If the stress is uniformly distributed, making σ a constant

$$\underline{\text{stress}} = \sigma = \frac{P}{A}$$

The stress causes an increase in length, $L_o + \delta$, and a slight decrease in diameter.

The linear average strain is

$$\underline{\text{strain}} = e = \frac{\delta}{L_o} = \frac{L - L_o}{L_o}$$

Strain is dimensionless since both δ and L_o are units of length.

Up to a limiting load the bar will recover its original dimension when the load is removed. This is

elastic behaviour

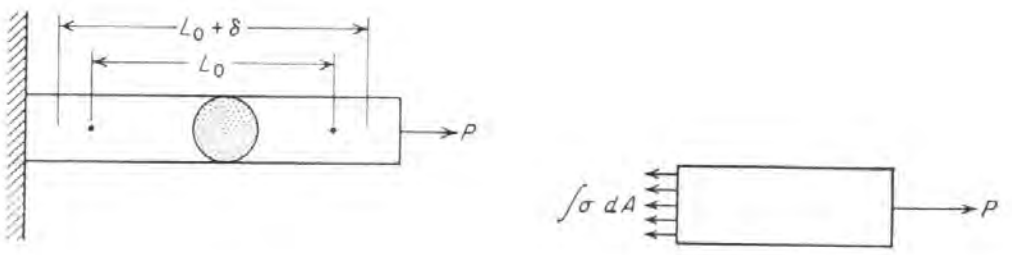

Figure 3-1: Cylindrical bar subjected to axial load

Beyond the limiting load the bar will experience a permanent change in dimension. This is

plastic behaviour

Up to the limiting load the deformation is proportional to the load. In this case the average stress and strain are related by

$$\text{Hooke's law: } \frac{\sigma}{e} = E = \text{constant}$$

where

E is the modulus of elasticity or Young's modulus (for zirconium alloys, the value of E is different in different directions).

For elastic deformation, a stress in the longitude direction causes a positive strain in that direction and a negative strain in the perpendicular or transverse direction. The ratio of the strains in the two directions is called

$$\text{Poisson's ratio} = \nu = \frac{transverse\ strain}{longitudinal\ strain}$$

The value of ν for metals is usually in the range of ν = .28 - .36 and for zirconium is taken as .33.

For Zircaloy tubing a similar parameter is sometimes used to express the ratio of axial strain to diametral strain when an axial stress is applied. This parameter combines both plastic and elastic strain, and is a variable depending on the crystallographic texture of the tubing and the amount of plastic strain applied.

$$\text{tubing contractile strain ratio} = \frac{diametral\ strain}{axial\ strain}$$

In practice, the distribution of stress and strain in a component is complex. Figure 3-2 shows the six components of stress that are needed to describe the state of stress at a point. Those stresses

acting normal to a surface are designated as normal stresses σ and those that act parallel to the surfaces are the shear stresses τ.

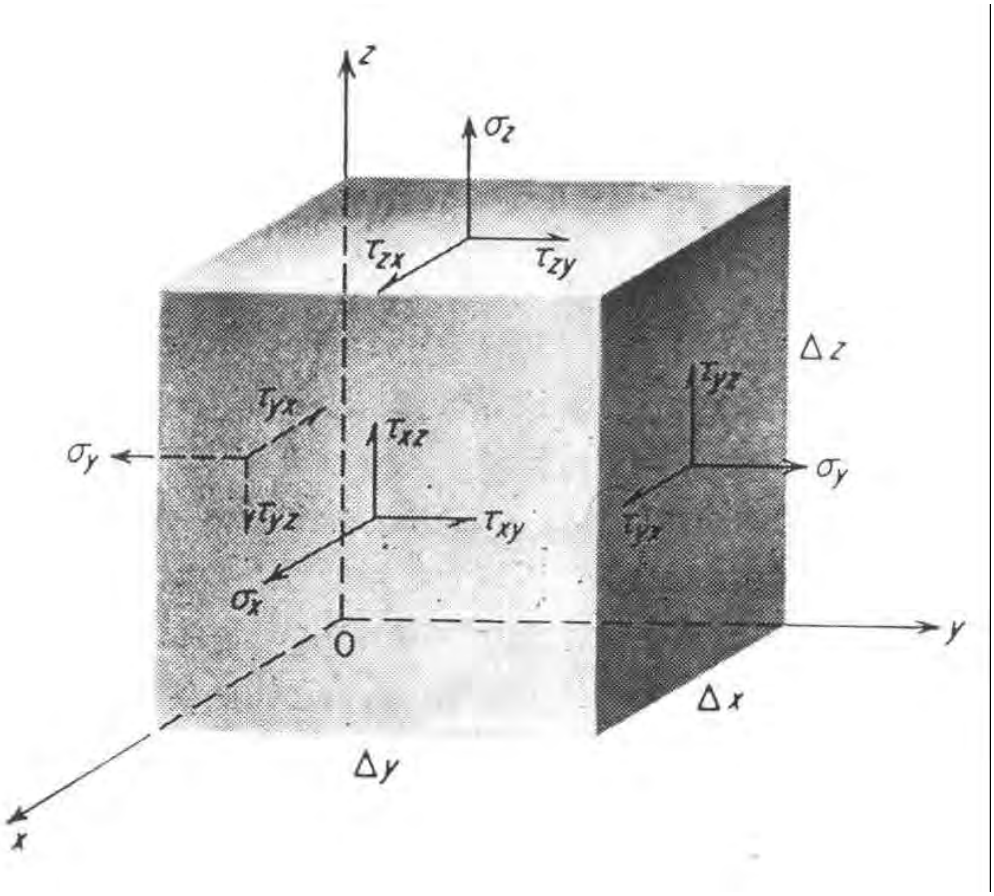

Figure 3-2: Stresses acting on an elemental unit cube

Although a rigorous analysis is beyond the scope of this review, several terms that arise often in discussion of analysis or testing are defined. A condition in which the stresses are zero in one of the primary directions is called

plane stress.

This condition is frequently approached in practice when one of the dimensions of the component or specimen is small relative to the others. Standard tensile specimens (discussed later) cut from, for instance, reactor components would be in plane stress. In Figure 3-2, plane stress results when

$$\sigma_Z = \tau_{ZX} = \tau_{YZ} = 0$$

Equilibrium requires that τ_{zx} and τ_{yz} also be zero, so the remaining stresses are the two normal stresses σ_x and σ_y and the shear stress τ_{xy}. Further analysis would show that in the case of plane

stress, a component would tend to fail at a 45° angle to the tensile stress axis, which is the location of the maximum shear stress.

In many practical applications, such as rolling or drawing, all displacements (strains) can be considered to be limited to one plane so that strains in the perpendicular direction are close to zero. This is known as a condition of

plane strain.

Since a plastic material tends to deform in all directions, even in a highly anisotropic one like zirconium, to develop plane strain it is necessary to constrain the flow in one direction. Figure 3-3, Ref. 11, illustrates that constraint can be produced by an external lubricated barrier such as the die wall in Figure 3-3a, or it can arise from a situation where only a part of the material is deformed and the rigid material outside the plastic region prevents the spread of deformation, Figure 3-3b. Deformation in cladding tubes is often considered to be in plane strain, because as the fuel pellet expands against the cladding wall, friction between the pellet and the cladding prevents the cladding from shortening in the axial direction. A simplified model of pellet-clad interaction (PCI) during a power ramp is given in Figure 3-3c, Ref. 12. In this case the cladding deforms in the circumferential and thickness directions, but not in the axial direction due to pellet-cladding friction. As discussed later, specimens intended for simulating cladding deformation must be able to approximate plane strain conditions.

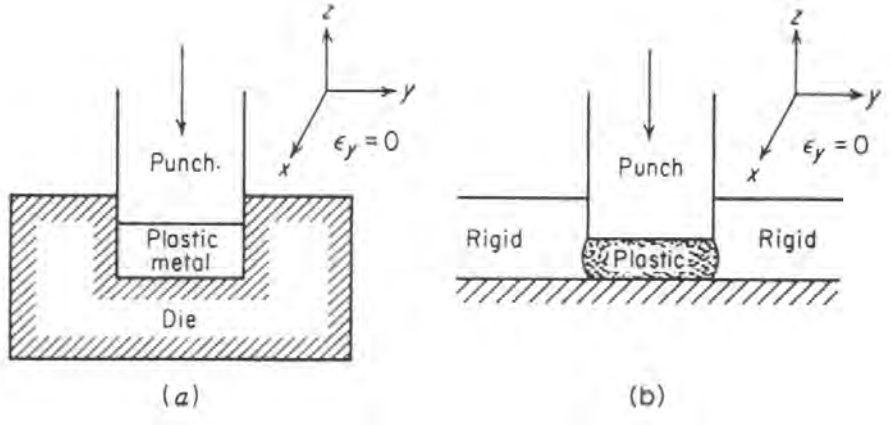

(a) (b)

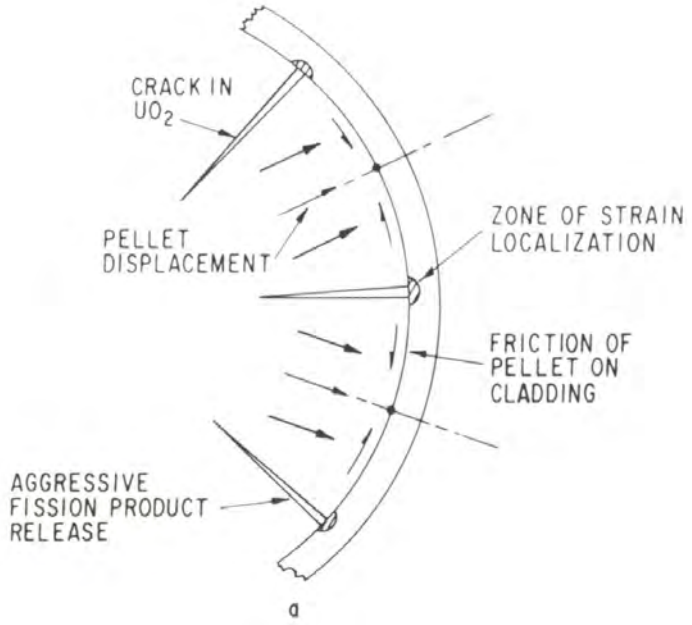

(c)

Figure 3-3: (a,b) Methods of developing plastic restraint, (c) An assumed model for pellet-clad-interactions

The terms principal stress or principal strains are used when discussing failure criterion, such as in section 1, Design and Performance Requirements. For our purposes it is sufficient to know that standard methods of mechanics of materials, as described in many textbooks like Ref. 11 and Ref. 13, are applied to obtain these stresses and strains. For any state of stress it is always possible to define a coordinate system which has axes perpendicular to the planes on which there are no shear stresses and which have the maximum normal stresses. These stresses are the principal stresses, specifically for conditions of plane stress. Standard mechanics of materials methods apply for zirconium alloys, but are complicated somewhat by the anisotropic nature of deformation in these alloys.

2.2 DISLOCATIONS

When materials scientists first realized that metals consisted of a regular array of atoms arranged in planes, they were able to calculate the stress needed to cause one plane of atoms to move one atom position relative to the adjacent plane of atoms. The stress required was about 10^7 psi (69,000 MPa), which is at least 100X greater than observed experimentally. The concept of a lattice defect, the dislocation, was therefore introduced to explain the discrepancy. It was shown theoretically that a dislocation could move through the crystal lattice at far less than the theoretical stress, and that it would produce a slip step, or a shear step, at a free surface.

Although it is not important for the purposes of this special topic report to examine dislocation theory, it will be helpful to review some basic geometries and terms. As indicated in Figure 3-4, a dislocation can be envisioned as an extra plane of atoms in the lattice. Because the interatomic

forces around the dislocation line are different than in a perfect lattice, the dislocation (in the illustrated case an edge dislocation) can move under the influence of an applied shear stress. When the edge dislocation reaches a free surface it does indeed cause a step at the surface. Figure 3-5, Ref. 11, illustrates the case of a dislocation, or group of dislocations, intersecting the surface of a copper single crystal. The basic phenomena are the same for Zircaloy.

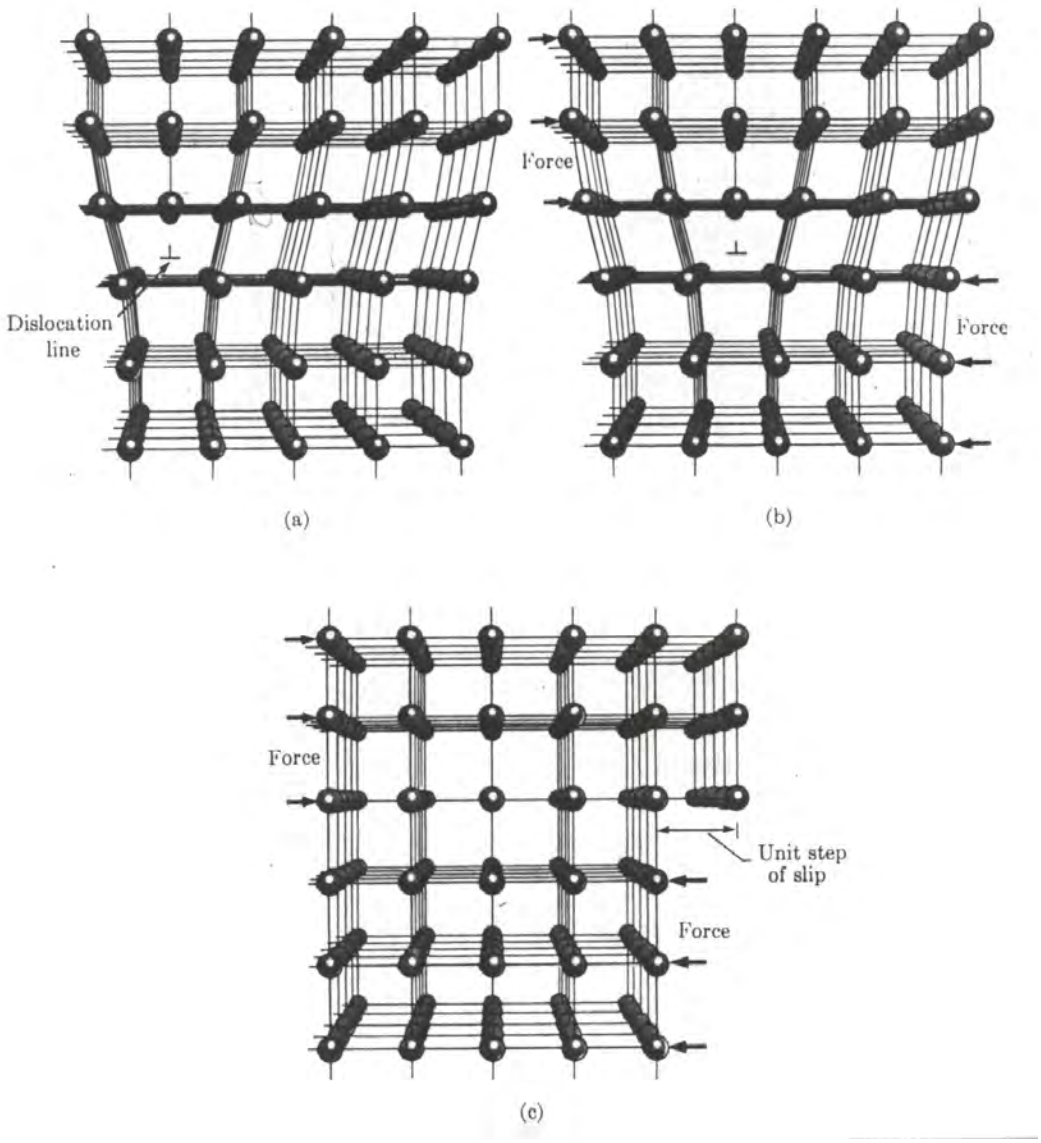

Figure 3-4: The motion of an edge dislocation and the production of a unit step of slip at the surface of the crystal. (a) An edge dislocation in a crystal structure. (b) The dislocation has moved one lattice spacing under the action of a shearing force. (c) The dislocation has reached the edge of the crystal and produced unit slip.

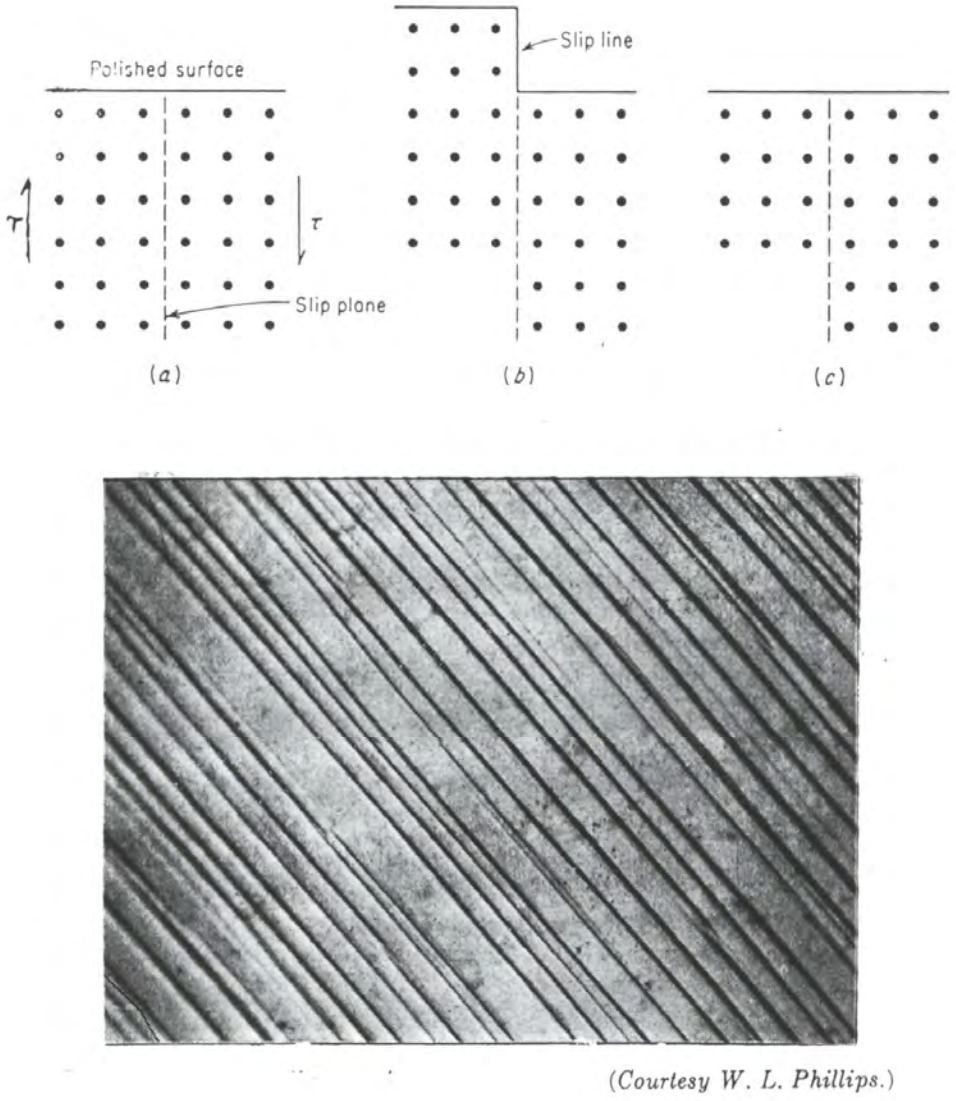

Figure 3-5: Schematic drawing of classical slip (above) and actual slip lines in copper, 500X (below).

When describing deformation or irradiation-induced defects, the term Burgers vector (**b**) is often used. Figure 3-6, Ref. 15, illustrates that b has a direction along the slip plane (perpendicular to the dislocation line in the case of an edge dislocation) and a magnitude close to that of one atomic spacing. If one takes a circuit around an atom in a perfect lattice, the circuit closes on itself, as in the lower portion of Figure 3-6. If a circuit is taken around an edge dislocation, the circuit does not close. The translation needed to close the circuit defines the Burgers vector, as in

the upper portion of the figure. The Burgers vector helps characterize irradiation-produced defects, as will be discussed later.

It has been convincingly shown that dislocations exist in metals and other materials. An example is shown in Figure 3-7, Ref. 11, where crystal planes are revealed by transmission electron microscopy. In metals the density of dislocations in a fully recrystallized (soft) material is on the order of 10^8 cm^{-2}. Deformation causes the moving dislocations to interact, resulting in two effects: 1) multiplication of the dislocaton density, to about 10^{12} cm^{-2} in fully cold worked materials and 2) increase in the resistance to free motion of the dislocations and an accompanying increase in strength (work hardening).

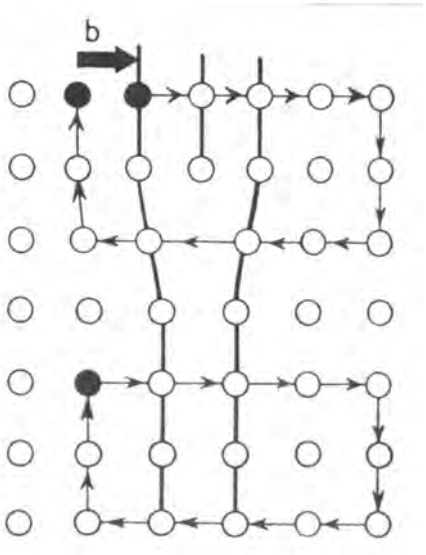

Figure 3-6: Burgers circuit around edge dislocation. The Burgers vector is b.

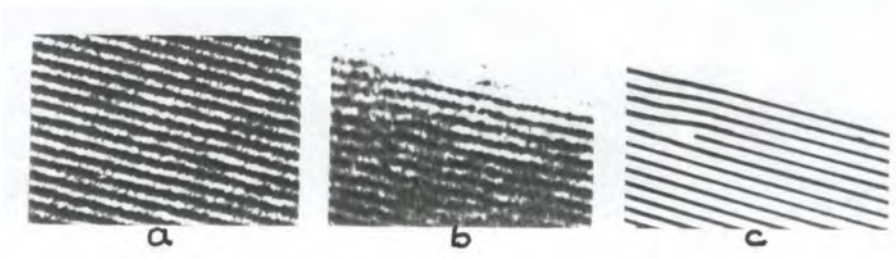

Figure 3-7: Electron Micrograph of dislocation in a crystal of plantinum phthalocyanine (X1,500,000). (a) Example of perfect array of crystal planes. (b) Perfect array interrupted by a dislocation. (c) Schematic drawing of (b) showing position of the dislocation.

Another class of defects which is important to the understanding of mechanical properties is the point defect. Some types are illustrated in Figure 3-8, Ref. 13. A substitutional impurity occupies a normal lattice site but is an atom of a different element than the bulk material. A vacancy is the absence of an atom at a normally occupied lattice site, and an interstitial is an atom occupying a

position between normal lattice sites. If the interstitial is of the same type as the bulk material, it is called a self interstitial and if it is of another kind it is called an impurity interstitial.

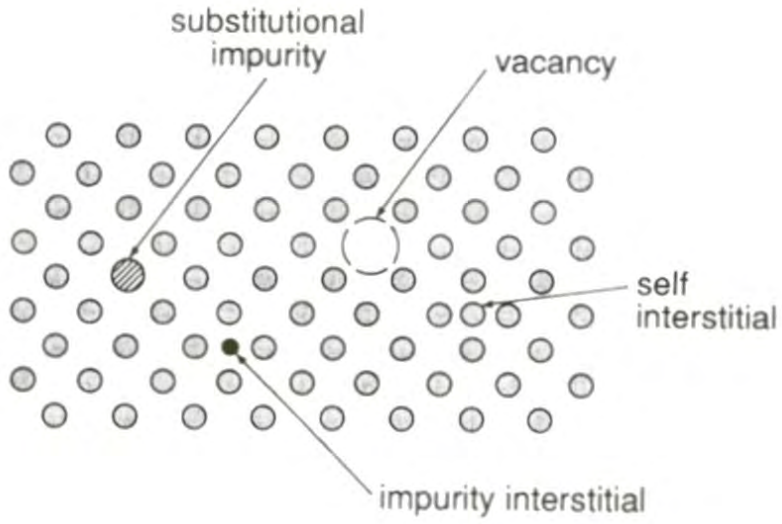

Figure 3-8: Four types of point defects.

Relatively small impurity atoms often occupy interstitial sites in materials with larger atoms. In zirconium alloys common interstitials are O, H, C, Fe, Cr and Ni. Common substitutional impurities (or alloying elements) are Sn and Nb.

It is seen in Figure 3-4 that the region around an edge dislocation is under stress due to the disruption of the normal lattice spacing there. As a result, this region strongly attracts vacancies, interstitials and self interstitials. For instance, for temperatures around 523K (300°C), oxygen in zirconium is strongly attracted to dislocations, and significantly affects the strength of unirradiated materials.

An important type of defect, particularly for irradiated materials, is the dislocation loop. If a significant number of vacancies or interstitials condense on a particular plane, a disk is formed with its boundary defined by a (circular) edge dislocation. This is illustrated in Figure 3-9 and Figure 3-10, Ref. 16. The Burgers vector b is perpendicular to the plane of the loop and therefore is the normal to the plane on which the loop lies.

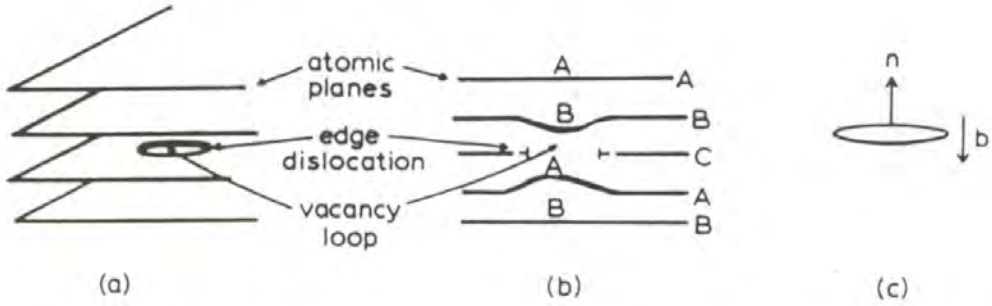

—The vacancy loop: (a) *Oblique view of a vacancy loop appearing as a disk on an atomic plane;* (b) *side view showing the change in stacking sequence through the loop;* (c) *orientation of the loop normal* $\vec{n}$ *to the Burgers vector* $\vec{b}$.

Figure 3-9: Vacancy loop

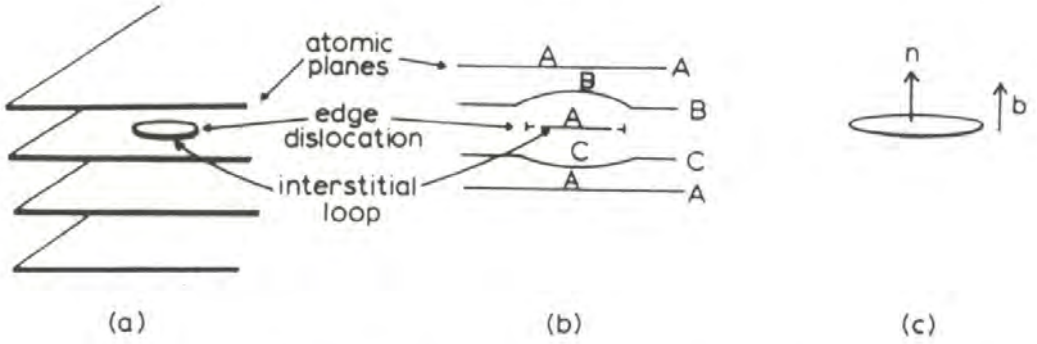

—The interstitial loop: (a) *oblique view showing the interstitial loop as a disk of atoms between atomic planes:* (b) *side view showing the change in stacking sequence;* (c) *orientation of the loop normal* $\vec{n}$ *to the Burgers vector* $\vec{b}$.

Figure 3-10: Interstitial loop

3.2. TEXTURE

Deformation in zirconium (and titanium) alloys is unique among the common structural materials in that properties are aniostropic, that is they are different in each direction of the material or component. Fabrication techniques intensify these differences, but anisotropy is inherent to zirconium because of its crystal structure. The zirconium crystallography is hexagonal close packed (HCP), as shown in Figure 3-11. Whereas the ratio of the orthogonal crystrallographic axes in cubic materials like steel, Inconel, brass, etc., is unity, in zirconium it is 1.59, with the c-axis larger than the a-axis. As a result, not only are mechanical properties such as strength and ductility anisotric, but also physical properties such as thermal expansion coefficients, thermal conductivity and elastic modulus. For the purposes of this review, the most important planes (noted in Figure 3-11) are two orthogonal planes, basal (0001) and prism $(10\bar{1}0)$, and a plane inclined to both of the above, pyramidal $(10\bar{1}2)$.

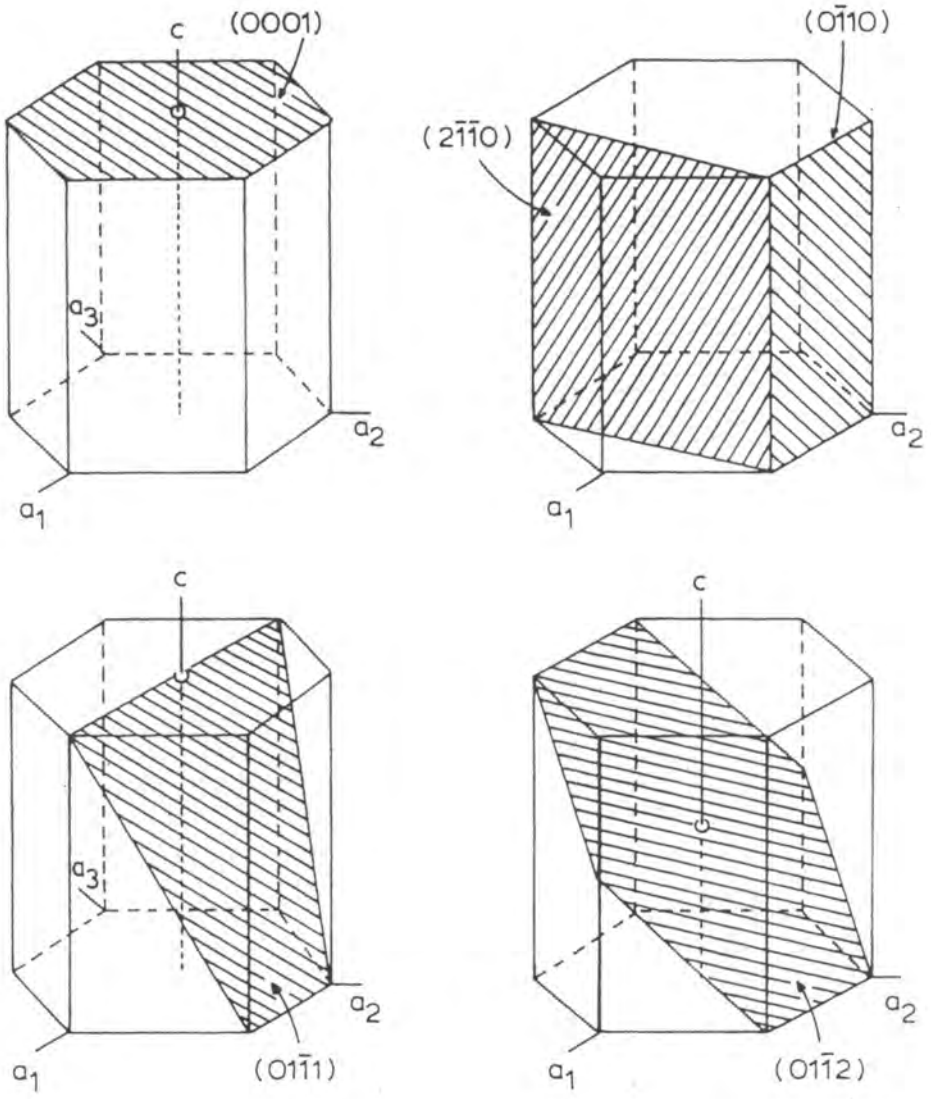

Figure 3-11: Some important planes in the hcp system in their Miller-Bravais indices. Prism plant ($01\bar{1}0$ or $10\bar{1}0$). Pyramidal ($10\bar{1}2$). Basal (0001).

To enable the degree of anisotropy to be predicted, the texture (eg., arrangement of crystallographic planes) of a specimen or component is usually expressed as an average distribution of basal (0001) planes in a particular direction of interest. X-ray diffraction techniques are used to obtain this distribution or the distribution of any plane of interest, Ref. 17. Figure 3-12, Ref. 18, shows the distribution of basal poles (normals to the basal plane) in various circumstances, with the usual distribution in Zircaloy tubing shown in Figure 3-12(e). More quantitatively, the distribution of basal poles is expressed by the Kearns texture parameter, f_x,

where f_x is the resolved volumn fraction of basal poles lying in the x-direction. The following definitions apply:

f_l = longitudinal (rolling, axial) direction

f_t = transverse (circumferential) direction

f_n = normal (radial) direction

$f_l + f_t + f_n = 1$

f = 0.33 implies randomly oriented basal poles.

In Figure 3-12 (b), $f_l = f_n = 0$ and $f_t = 1$

In Figure 3-12 (d), $f_l = f_t = 0$ and $f_n = 1$

In Figure 3-12 (c), $f_l = f_n = f_t = .33$

In Figure 3-12 (e), showing a typical texture in Zircaloy tubing, $f_l = 0.07$, $f_t = 0.33$, $f_n = 0.60$

In a typical rolled plate $f_l = .2$, $f_t = .3$, $f_n = .6$.

A detailed account of texture-related deformation in zirconium alloys is given by Tenckhoff, Ref. 19, a summary of which is given in Appendix A and in Ref. 20.

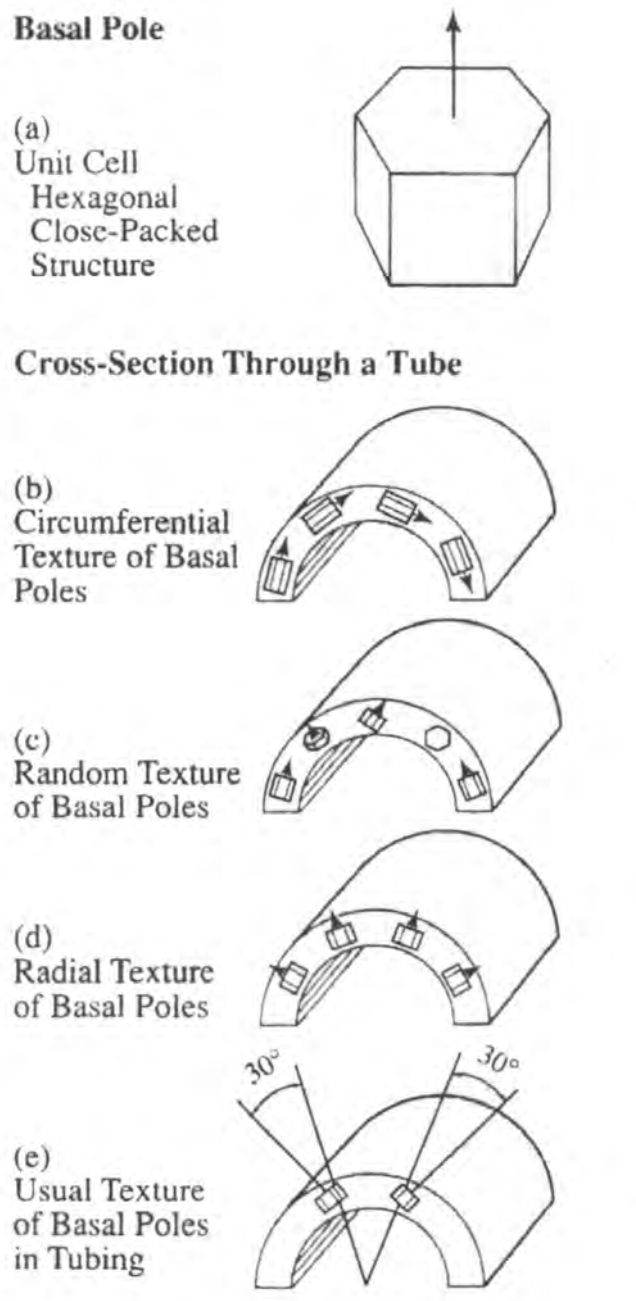

Figure 3-12: Illustration of crystal textures in tubing.

3.3. IRRADIATION DAMAGE

Performance of nuclear materials is often judged as a function of time in a reactor, or as a function of exposure to the reactor environment. To the materials analyst an important unit of exposure is neutron fluence, or the number of neutrons that have passed through a unit area of material, n/cm^2 or n/m^2. Since the amount of "damage" done by neutrons depends on the energy of the neutron, it is necessary to specify the neutron energy of record. Since more "damage" is done by high energy or "fast" neutrons, the most common unit is for energies greater than 1 MeV, fluence ≡ n/m^2 (E>1 MeV).

However, sometimes a lower energy is noted, fluence ≡ n/m^2 E>0.1 MeV.

For light water reactors (BWR and PWR) a rule of thumb is that

$2+n/m^2$ (E>0.1 MeV) is about 1 n/m^2 (E>1MeV).

However, for fast reactors of the BOR60 type used in Russia the relationship is closer to:

$4+n/m^2$ (E>0.1 MeV) is about 1 n/m^2 (E>1MeV).

Detailed comparisons, of course, must be based on detailed analysis of the neutron energy spectra of reactors of interest. If the complete energy spectrum is considered and consistent estimates of the neutron energy needed to "knock" an atom from its normal lattice position are used, it is helpful to use displacement per atom, dpa, as the measure of irradiation damage. DPA refers to the average number of times an individual atom is displaced from its normal lattice position during a given reactor exposure. For zirconium alloys the value commonly used is (Ref. 21):

$$1 \text{ dpa} = 4.5 \times 10^{24} \text{ n/m}^2 \text{ (E>1 MeV)}.$$

For reactor engineers the most important unit of exposure is fuel burnup. This is usually expressed as

exposure ≡ GWd/MT or MWd/KgU.

The conversion of burnup to a neutron fluence is complex, depending on neutron-energy spectrum, fuel enrichment, and other factors. But for a rule of thumb, it is usually close to use:

$$10 \text{ GWd/MT is about } 2 \times 10^{25} \text{ n/m}^2 \text{ (E>1 MeV)}.$$

It is therefore seen that an end-of-life exposure of

50 GWd/MT

is equivalent to

$$1 \times 10^{26} \text{ n/cm}^2 \text{ (E>1 MEV)}$$

or

20 dpa.

This means that on the average each atom has been displaced from its normal lattice site about 20 times! No wonder properties are expected to change with reactor exposure.

Under thermodynamic equilibrium, all metals contain a certain number of defects – vacancies, interstitials, dislocations. Under irradiation, many more defects are created by elastic and non-elastic collisions between the radiation particles and irradiated metal. The most simple type of irradiation-produced defect is the Frenkel pair, which is the vacancy-interstitial pair that is formed when an atom is knocked from its normal lattice position (forming a vacancy) and lodges itself in an interstitial position nearby in the lattice (forming a self-interstitial). A more complicated but transient form of damage results when many atoms are displaced locally, shown in Figure 3-13, Ref. 22 as a displacement spike (which is a form of what is sometimes termed a thermal spike). In this case many atoms have been forced into interstitial sites surrounding a hollow core. This configuration is not stable, however, and quickly converts to the situation shown in Figure 3-14, Ref. 16, which is a damage zone with a vacancy rich core and an interstitial shell. This configuration is also not stable, as the vacancies and interstitials prefer to migrate to sinks such as grain boundaries and dislocations. Importantly, many of the vacancies combine together in planar arrays to form the vacancy dislocation loops shown in Figure 3-9, and the interstitials do likewise to form interstitial dislocation loops, Figure 3-10.

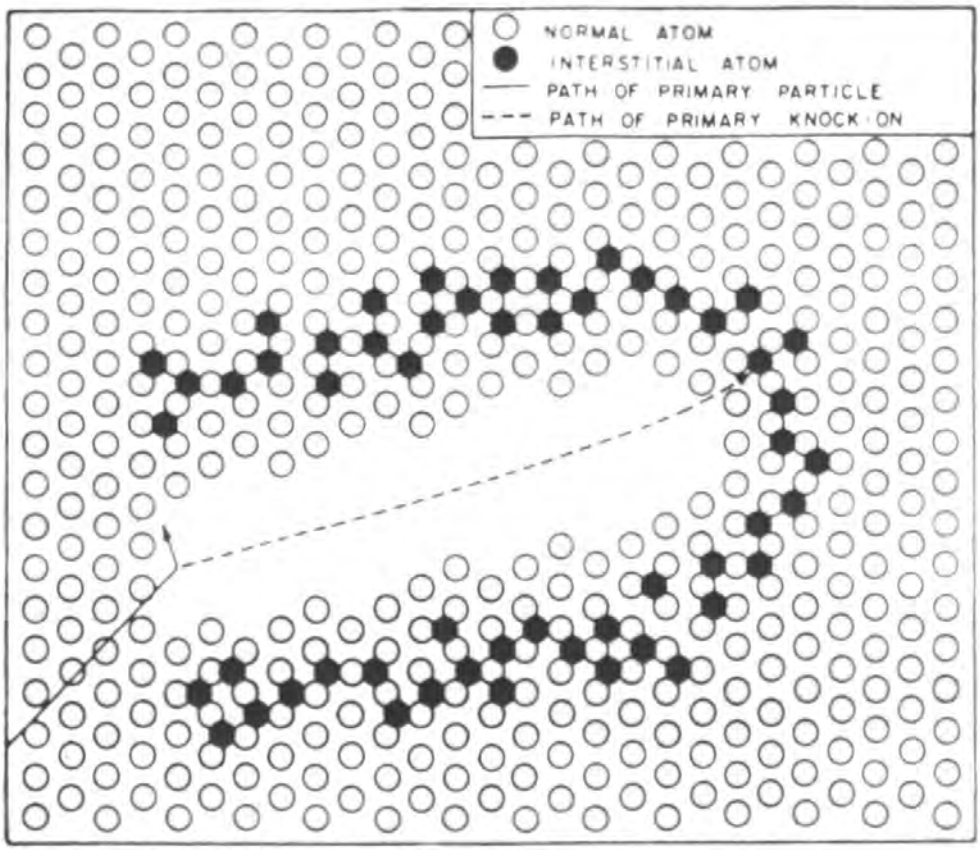

Figure 3-13: Schematic drawing of a (Brinkman) displacement spike.

4. TENSILE DEFORMATION

4.1. TESTING

Chapter 2 outlines requirements for operation and general fabricability of various reactor components. In many cases the properties can be defined and obtained experimentally by a tensile test, often a simple uniaxial test. A typical system for conducting such tests is illustrated in Figure 4-1 [Ref. 13]. Older systems, not shown, are mechanically driven by large screws, while the illustrated system uses an oil-pressurized piston. The older screw-driven machines have the advantage of providing a controllable, steady strain, while the newer servohydraulic machines are quite sophisticated, able to provide variations in load or strain patterns.

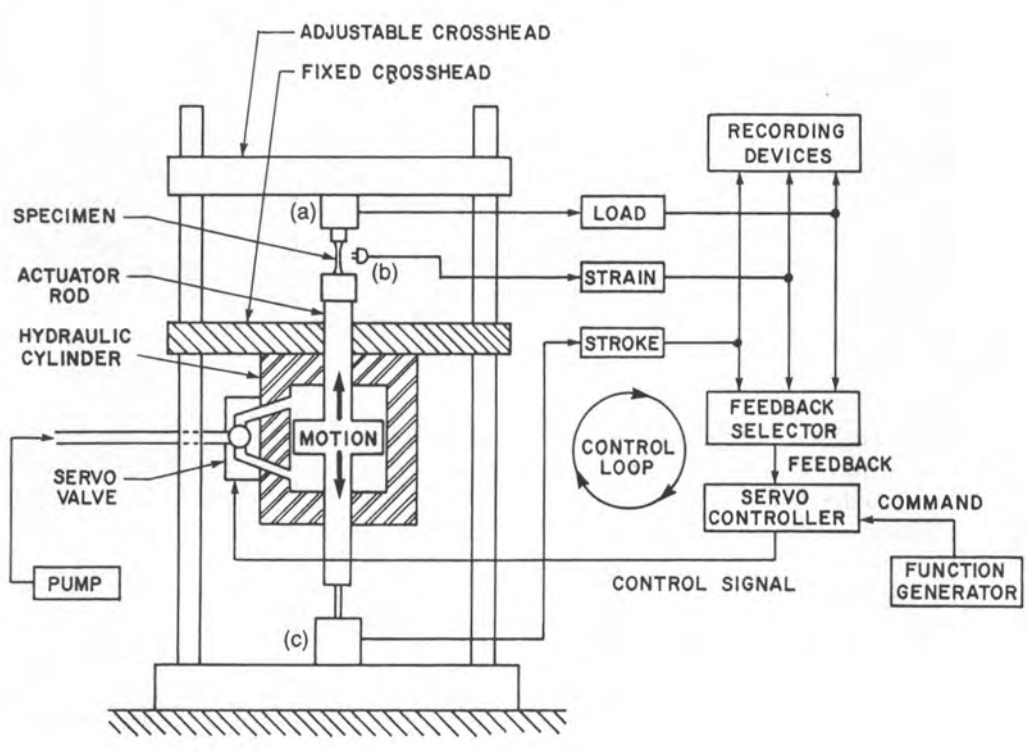

Figure 4-1 Modern closed loop servohydraulic testing system. Three sensors are employed: (a) load cell, (b) extensometer, and (c) LVDT.

The test systems themselves usually do not measure specimen strains directly except by providing carefully controlled and measured motion of the specimen grips. There are many methods used to grip specimens for testing. For standard plate or sheet specimens, ASTM E-8 recommends wedge grips like those shown in Figure 4-2**.** For Zircaloy reactor components the specimen design and gripping systems are often not standard, as discussed later.

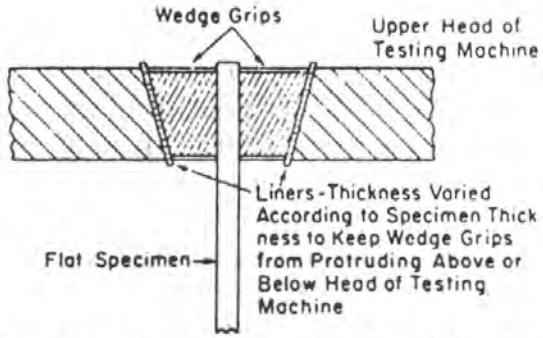

FIG. 2 Wedge Grips with Liners for Flat Specimens

Figure 4-2 Wedge grips with liners for flat specimens.

4.2. STRESS-STRAIN BEHAVIOR-UNIRRADIATED MATERIAL

A standard engineering stress-strain curve is shown in Figure 4-3, with common terms for important parameters designated. A good description of stress-strain behavior and terms given by Dowling [Ref. 13] is paraphrased below. (For our purposes the symbols for strain, ε and e, are both used to mean engineering strain, although a strict interpretation would usually result in ε being defined to mean true or instantaneous strain, $\varepsilon = \ln(1+e)$.):

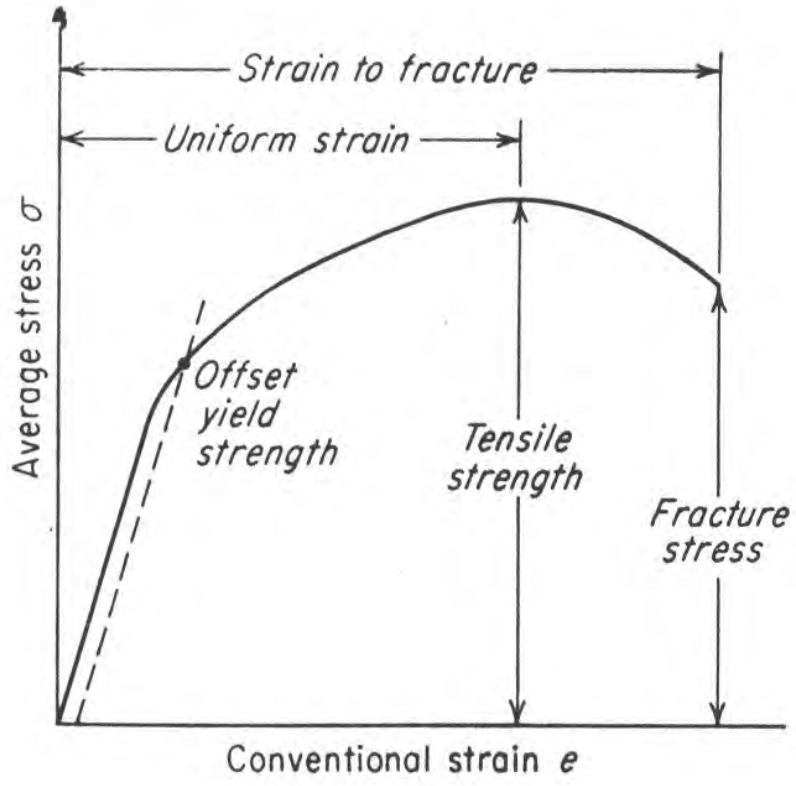

Figure 4-3 The engineering stress-strain curve.

The *ultimate tensile strength,* σ_μ, also called simply the *tensile strength*, is the highest engineering stress reached prior to fracture. If the behavior is brittle, the highest stress occurs at the point of fracture. However, in ductile metals, the load, and hence the engineering stress, reaches a maximum and then decreases prior to fracture, as in Figure 4-3**.** In either case, the highest load reached at any point during the test, P_{max}, is used to obtain the ultimate tensile strength by dividing by the original cross-sectional area.

$$\sigma_\mu = \frac{P_{\max}}{A_1} \tag{4.4}$$

The *engineering fracture strength,* σ_f, is obtained from the load at fracture, P_f, even if this is not the highest load reached.

$$\sigma_f = \frac{P_f}{A_1} \tag{4.5}$$

Hence, for brittle materials, $\sigma_\mu = \sigma_f$, whereas for ductile materials, σ_μ may exceed σ_f.

5. OTHER IMPORTANT TESTS

This section discusses a variety of tests related to obtaining mechanical properties of zirconium alloy components. These tests are important during processing of zirconium fabrication of components, qualification of components, and reactor service. The treatment here is less detailed than for sections 2, 3, 5 and 6, but includes enough fundamental information to allow one who is not often involved in these areas to evaluate data or information in the specific areas covered.

5.1. HARDNESS

Hardness of a material is a rather ill-defined term. It is related to strength and ductility, to resistance to plastic deformation, to wear resistance; however, it is most commonly defined as resistance to indentation. All of the hardness tests evaluate indentations in one way or another.

Hardness is often used as a quality control tool during production of material and components. It is usually made a material specification by the vendor, not because it is a key property in itself, but because it can be related to grain size, chemistry (particularly contamination by oxygen or nitrogen), heat treatment, cold work, etc. It cannot identify a specific property uniquely but can serve as a warning flag that something is not right. Hardness also is useful for examining deformation mechanisms important to the understanding of component performance, and in many cases is easier to use than other methods. Although elevated-temperature (hot) hardness techniques and equipment are available, they are not often used. In the discussion below, we will consider only tests at nominal room temperature.

5.1.1. Hardness Tests

A variety of tests are commonly used. The most useful are discussed here. They each use an indenter of a unique shape and a hardness number is calculated using the amount of deformation which is produced by a given applied load on the indenter. They all require careful surface preparation if the data is to be reproducible and of high quality. The “macro-tests” are most robust and useful for less-than-ideal conditions; the “micro-tests” require strict attention to specimen preparation details (eg., specimen flatness, smoothness, uniformity).

Since plastic deformation occurs during hardness testing, there is some relationship of hardness to tensile or compressive properties. Deformation under the indenter, however, is complex and the relationship is not straightforward. However, it is generally accepted that hardness of steels is most closely related to the tensile strength (UTS). For irradiated Zircaloy, this would seem to be true. For unirradiated Zircaloy, it is not clear whether the yield stress or UTS is more appropriate.

Figure 5-1 [after Ref. 13] gives a rough idea of the hardness of zirconium and Zircaloy relative to other materials. The range for each starts with unirradiated recrystallized material and goes to irradiated or cold worked material. Literature data were used for Zircaloy [Ref. 111**,** Ref. 79] and zirconium [Ref. 111], and of course these values depend on texture and other variables.

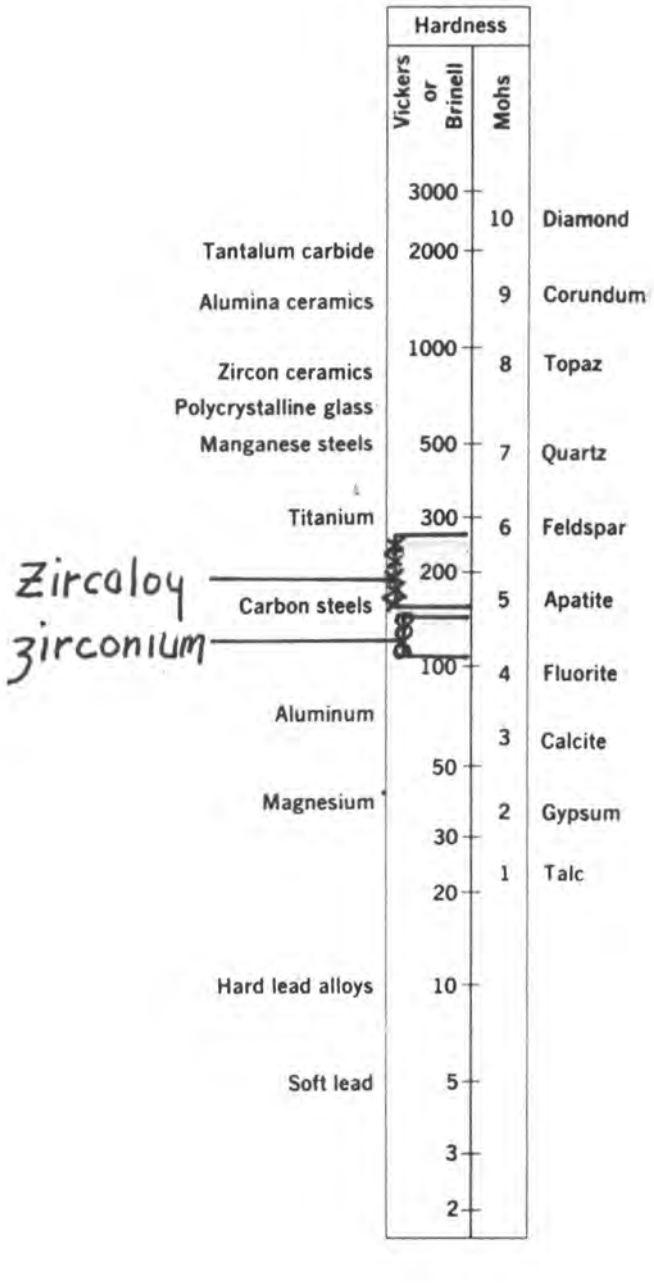

Figure 5-1 Approximate relative hardness of various metals and ceramics. The approximate ranges for unirradiated/irradiated Zircaloy and zirconium are added.

5.1.1.1.1 Macro-hardness

Rockwell Hardness, RHX

Rockwell is perhaps the most robust and most used hardness test. It uses a diamond cone or a steel ball as the indenter, and uses the depth of indentation under a constant load as the measure of hardness. It uses a two stage loading, which minimizes the amount of surface preparation needed. A minor load of 10 kg is applied first to overcome any surface irregularity, followed by the major load. Various combinations of indenters and major loads are used for suitable hardness ranges; therefore a Rockwell hardness must be reported with the particular combination identified. Thus, HRA, HRB, HRC, etc., are all Rockwell hardnesses with the specific A, B, and C combinations of load and indenter. The hardness ranges overlap, and the right combination can produce a small or large indentation, as desired.

Calibration of the testing apparatus utilizes a standard test block of known hardness.

Brinell Hardness, HB or BHN

The Brinell hardness test was proposed in 1900 and is still being used. It consists of indenting the surface with a 10 mm-diameter steel (or tungsten carbide) ball with a large 3000 kg load. Variations of the ball size and load can be made, but in general the HB is constant only for a given applied load and ball diameter. The HB is obtained by measuring the diameter of the indentation and calculationg the ratio of the applied load to surface area of the indentation. HB and RH are widely used in industry and in zirconium production facilities, but have limited use in zirconium alloy components where the component thicknesses are small. A typical Brinell hardness testing machine is shown in Figure 5-2 [Ref. 13].

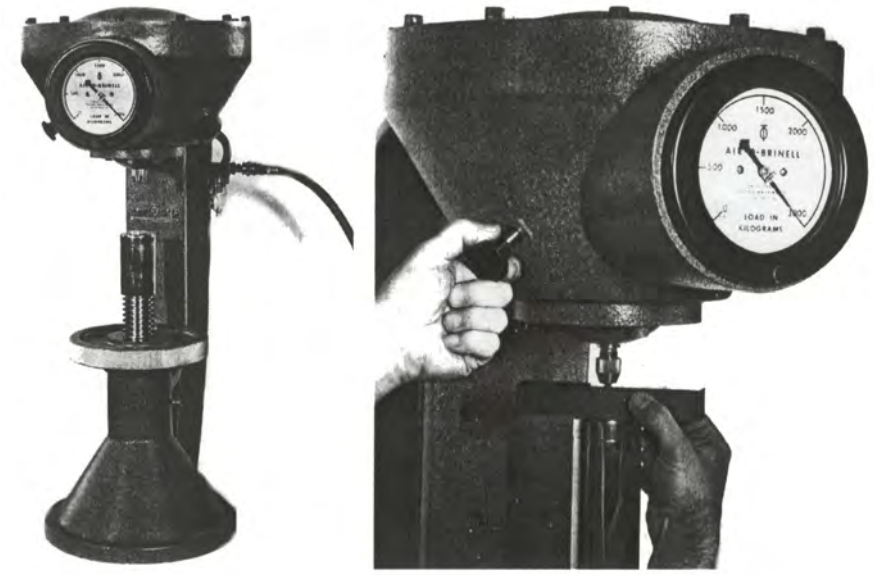

Figure 5-2 Brinell hardness tester, and indenter being applied to a sample.

6. FATIGUE

6.1. INTRODUCTION

Components of reactors and many other machines and structures are often subjected to alternating or cyclic loads. Utilities are sometimes required to do grid load following and frequency control operating conditions, resulting in fuel temperature fluctuations caused by differential thermal expansion between pellets and cladding. In addition, complex thermohydraulics within the reactor create conditions of oscillating pressures and loads. The cyclic stresses and strains thus created and accumulated over a number of cycles can create microscopic damage in Zircaloy that lead to macroscopic cracking of components. These phenomena, due to cyclic stressing which can occur at stresses considerably below the ultimate tensile stress, are called fatigue. The term itself originated in the mid-1800's, as engineers noted that parts such as rotating axles in wagons gradually lost their resistance to stresses, and after long operation failed suddenly.

Unlike many other technologies where fatigue failures account for large percentage of all mechanical failures, in practice, reactor components have not been particularly susceptible to fatigue failures. In specific testing programs, for instance, no negative effects on fuel rod performance were observed after extensive power cycling in a test reactor Ref. 26. The USNRC Standard Review Plan Ref. 2 states, however, that the cumulative number of strain fatigue cycles on structural members (grids, guide tubes, fuel rods, channels, etc.) should be significantly less than the design fatigue lifetime, which must be based on appropriate data and include a safety factor of 2 on stress amplitude or 20 on the number of cycles. "Appropriate data" means either the data of Ref. 8 (to be discussed later) or other data justified and approved by NRC.

There are three major approaches to analysing fatigue. The traditional approach is based on analysis of the nominal or average stress in the component, as modified by the effects of stress raisers such as holes, fillets, interfaces, etc. This is the stress-based approach. The strain-based approach involves a more detailed analysis of the plastic and elastic strains that develop in the component of interest e.g. Ref. 27. The third is the fracture mechanics approach, which is considered in general terms in another section of this report. The other two approaches are discussed here.

6.2. STRESS-BASED FATIGUE

Figure 6-1 illustrates typical stress-based fatigue cycles. Figure 6-1a illustrates a completely reversed sinusoidal stress, such as could be produced by a rotating shaft. In this case the magnitudes of the minimum and maximum stresses are equal. Figure 6-1b gives the case where the magnitudes of the minimum and maximum stress are not equal. In this case both are tension, but they could have opposite signs as well.

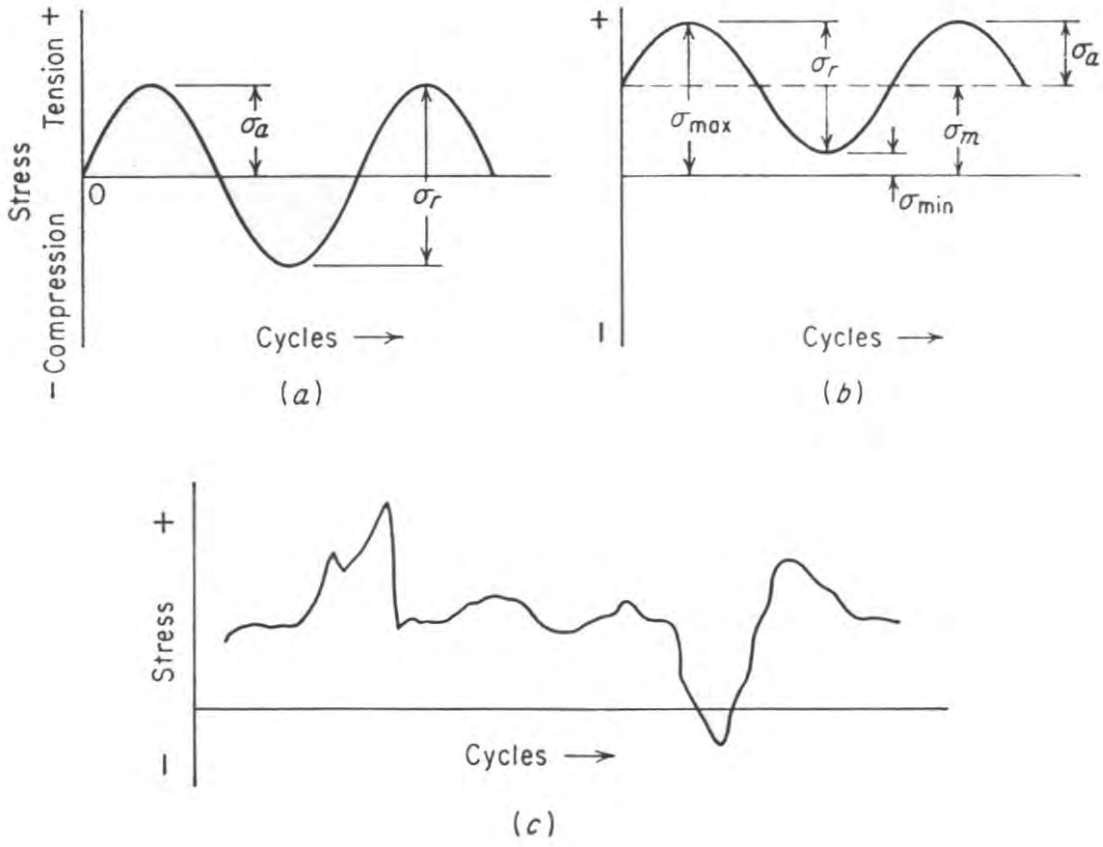

Figure 6-1 Typical fatigue stress cycles. (a) Reversed stress; (b) repeated stress; (c) irregular or random stress cycle

The stress ratio, R, is defined as the ratio of the minimum to maximum loads, $\sigma_{min}/\sigma_{max}$. Several types of loading are illustrated by static loading, R = 1; tensile cycle loading, 0<R<1; reversed load cycling, -1<R<0; symmetrical load cycling, R = -1.

Figure 6-1c illustrates a complicated stress cycle, which could be induced, for instance, in a component by thermohydraulic-induced vibration. Some useful terms for these cases are included in Table 6-1.

Table 6-1: Useful terms relating to fatigue

stress range,	$\Delta a = \sigma_{max} - \sigma_{min}$
mean stress,	$\sigma_m = (\sigma_{max} + \sigma_{min})/2$
stress amplitude	$\sigma_a = \Delta\sigma/2$
alternating stress	$\sigma_a = \Delta\sigma/2$
stress ratio	$R = \sigma_{min}/\sigma_{max}$
fatigue (endurance) limit	E_l = stress below which fatigue failure does not normally occur
fatigue strength	= stress amplitude value from S-N curve at a particular life of interest
high cycle fatigue	= when fatigue life is greater than about 10^6 cycles
low cycle fatigue	= when fatigue life is below about 10^5 cycles
strain amplitude	$\varepsilon_a = \frac{\Delta\varepsilon}{2}$
number of cycles to failure	$= N_f$
plastic strain	$= \Delta\varepsilon_p$ = width of hysteresis loop
plastic strain amplitude, E_{ap}	$= \Delta\varepsilon_p/2$

The standard method of presenting stress-based fatigue data is by the stress vs number of cycles to failure (S-N) curve, illustrated in Figure 6-2. The cycles-to-failure (N) axis is usually in log form, while the stress axis is given either in linear or log form. Figure 6-2 illustrates that some materials have a fatigue limit, that is, below a given stress they will not fail in fatigue. Interest in Zircaloy is mostly for less than a few million cycles, and it appears that there may be a fatigue limit in that range. As a rule of thumb, the fatigue limits of many ductile materials is less than half of the ultimate tensile stress. This observation is quite dependent on microstructure, and does not hold, for instance, for both unirradiated and irradiated Zircaloy. In general S-N curves are affected by material, specific material microstructure, geometry (like notches), surface finish, chemical and thermal environment, frequency of cycling, residual stress, and mean stress Ref. 28.

7. FRACTURE TOUGHNESS

7.1. BASICS

Zircaloy components are fabricated to be “defect free”; however, in practice these components, as do all engineering components, can have defects in the form of small cracks. Such cracks can originate during fabrication or during in-reactor service. The questions that arise are “how easily will the crack propagate?” and “will the crack compromise safe operation of the component?” To provide answers to such generic questions, a new technology/science has been developed – fracture mechanics. Extensive employment of fracture mechanics to cracking issues in steels and other high strength alloys has resulted in increased safety in pressure vessels, aircraft engines, building structures and many other commercial and military applications. Use of fracture mechanics technology for reactor Zircaloy issues has been limited in the past. This is partly due to a lack of regulatory emphasis on cladding failure as a safety issue Ref. 2 and to the fact that, as explained below, much of the standard fracture mechanics methodology does not apply to standard PWR and BWR bundle component geometrics. However, as higher burnup increases the probability of operation with defects present and as new zirconium alloys are introduced, the use of fracture mechanics to predict the behavior of cracks or defects is increasing. Papers at recent international conferences have illustrated fracture mechanics techniques for analyzing crack propagation in failed Zircaloy tubing, Ref. 56, Ref. 57 and, Ref. 58. And for many years, leak-before-break criteria and critical crack lengths in CANDU-type pressure tubes have been analyzed, with considerable success, using fracture toughness methodology, Ref. 59, Ref. 60 and, Ref. 61.

It is known that a small crack in a large member can substantially alter the stress distribution and magnitude near the crack. This is illustrated in Figure 7-1, where it is seen that the stress at the edge of the crack, parallel to the applied stress, is many times higher than the nominal applied stress. In fact as the radius of the crack tip approaches zero, the stress there would approach infinity.

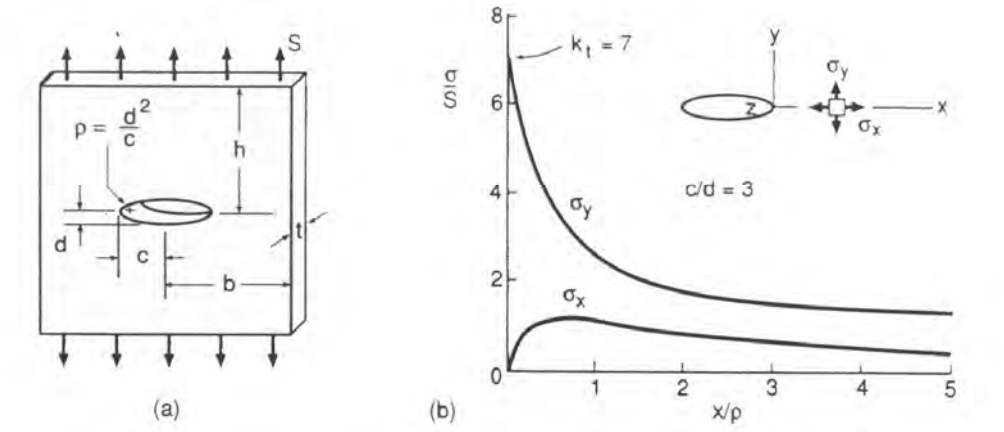

Figure 7-1 Eliptical Hole in a Wide Plate Under Remote Uniform Tension and the Stress Distribution Along the x-axis Near the Hole for One Particular Case, Ref. 28.

However, in a ductile material like Zircaloy, the stress at the crack tip is relieved by plastic deformation, so the local stress does not go to infinity. A plastic zone develops, Figure 7-2, in which the stresses are strongly influenced by the crack tip. If the size of the plastic zone is not "too high" (to be quantified later), the theory of linear-elastic fracture mechanics (LEFM) can be used to determine what combination of crack size, crack and component geometry, and applied stress will result in component operation without danger of rapid crack propagation. Of course the details of LEFM are well beyond the scope of this review, but the basic features as applied to Zircaloy component behavior will be described here.

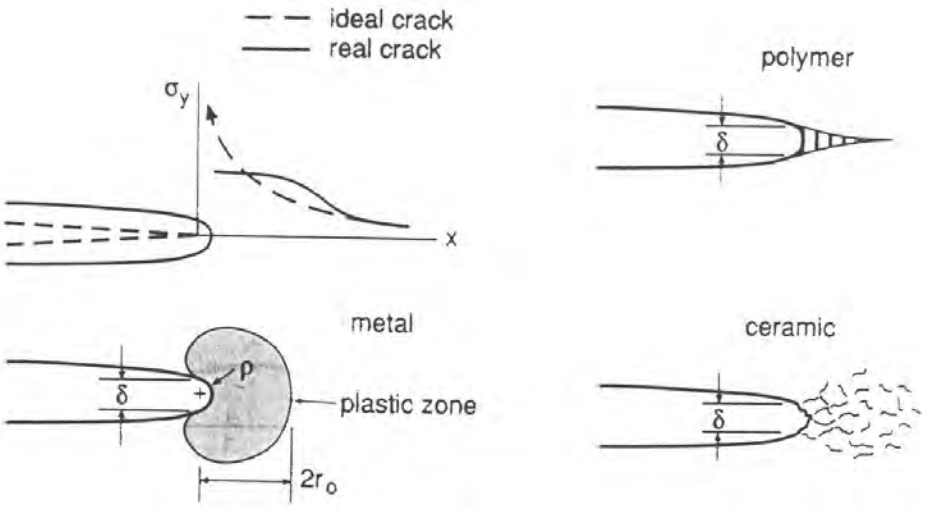

Figure 7-2 Finite stressesand nonzero radii at tips of cracks in real materials. A rediopn of intense deformation forms due to plasticity, crazing, or microcracking, Ref. 28.

A basic feature of LEFM is the stress intensity factor, K, which is a function of the applied stress, *S*, the crack length, *a*, and a crack and specimen geometry factor, *g*.

When the value of K is below a critical value, K_c, a given material can resist rapid crack propagation or brittle fracture. This K_c is called the fracture toughness. As illustrated in Figure 7-3, K_c is usually a function of material strength, and is also a function of the material or specimen thickness, Figure 7-4.

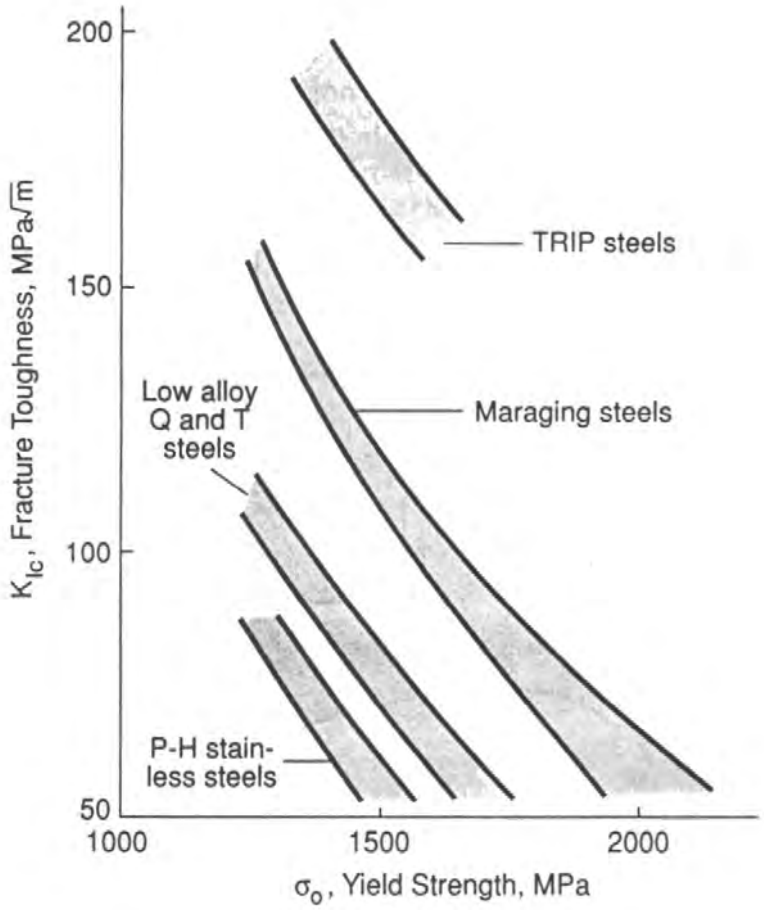

Figure 7-3 Decreased Fracture Toughness, as Yield Strength is Increased by Heat Treatment, for various Classes of High-Strength Steel, Ref. 28.

8. WRAP-UP

Six sections of this report describe the role of mechanical properties of zirconium alloys in attaining successful operation of the fuel bundle in a light water reactor. Specific mechanical properties are required for fabrication of components and for safe and efficient operation.

ASTM Specification B811-97 prescribes certain values for chemistry, grain size, corrosion resistance, tensile mechanical properties, and hydride orientation. In addition,. optional specifications are given for burst test properties and contractile strain rates. Also, test techniques are specified. As described in section 2 of this report, maximum stresses and strains are specified by USNRC, and a specific fatigue limit is given. Guidance is provided on fretting wear, dimensional stability, creep and ballooning under off-normal conditions, cladding collapse and strain during pellet cladding interactions (PCI).

To address the various issues, this report addresses several topics in detail; however, section 3 starts with a general description of various basic phenomena. Included are deformation principles, crystallographic uniqueness of zirconium alloys, and an introduction to irradiation effects on microstructure. The basics can be related to specifics given in later sections.

Details of tensile deformation given in section 4 are important to both fabrication and performance issues. Tensile testing is probably the most straightforward of the mechanical testing techniques and is widely used to evaluate fabrication issues and as-irradiated behavior of all components. The many factors which affect interpretation of tensile test results include irradiation, texture, specimen geometry, stress states, alloy content, and hydrogen concentration and distribution. With an understanding of those details, interpretation of test and performance results is facilitated.

Other tests important for specific reasons are reviewed in section 5. Knowledge of creep behavior is essential to assess in-reactor dimensional stability issues of fuel rods, control rod guide tube assemblies, spacer springs, and channels. Although the mechanisms of in-reactor creep are beyond the scope of this review, section 4 reviews the basics of creep deformation to facilitate analysis of the various experimental studies of in-reactor creep that are now in progress.

Section 5 also gives details of hardness testing and analysis. This relatively simple test has proven to provide important information on in-reactor component performance as well as serving as an indicator of quality problems during manufacturing.

Although burst strength and ductility are sometimes used in fabrication quality control, this type of test is perhaps more useful to obtain properties of irradiated tubing since the test parameters are similar to those experienced by fuel cladding in-service. It is a difficult test to conduct, as many variables can affect the results. This test is also described in section 5.

Fatigue properties are one of those specified by the US NRC. Fatigue stressing can occur in reactor due to flow-induced vibrations, but the main source is thermal cycling, particularly in fuel rods. Although it is doubtful that fatigue failures have actually occurred in reactor components, considerable effort has been spent to determine fatigue lives and strain limits. Section 6 attempts a thorough review of basic fatigue phenomena and experimental data. All of the data gathered since the NRC-imposed fatigue strength requirements have shown that the fatigue limit is conservative.

The final section deals with a topic only recently considered important for component performance. Fracture toughness has been hypothesized as the cause of the long split cladding problem experienced in BWRs in the 1990's. Although it has been shown with fair certainty that this hypothesis was not correct, useful developments relevant to thin-walled cladding behavior have resulted from the long-split investigations. Techniques to evaluate fracture toughness of cladding, not previously available, are actively being developed. Section 7 describes fracture toughness issues in general and thin-wall tubing techniques in particular.

It is intended that use of this document will facilitate both practical and mechanistic understanding of the topics covered. It is meant to be a useful guide for application to design and performance issues, and a reference from which critical review of published papers and presentations will result.

9. REFERENCES

Ref. 1 **10 CFR Part 50, Appendix A, "General Design Criteria for Nuclear Power Plants", NRC.**

Ref. 2 **US Nuclear Regulatory Commission Standard Review Plan, NUREG-0800, Office of Nuclear Reactor Regulation, 1981.**

Ref. 3 **10 CFR Part 100, "Reactor Site Criteria", NRC.**

Ref. 4 **10 CFR Part 50, §50.46, "Acceptance criteria for emergency core cooling systems for light water nuclear power reactors", NRC.**

Ref. 5 **"Rules for Construction of Nuclear Power Plants Components", ASME Boiler and Pressure Vessel Code, Section III, 1977.**

Ref. 6 **"Sickerheitstechnische Regel des KTA", Abschaltsystem von Leichtwasserreaktoren, KTA 3103, Anhang B, Carl Heymanns Verlag KG.**

Ref. 7 **A. Hotta, "BWR Fuel Rod New Design Methodology", TSI report: TCMR-95 033, Rev. 0, 1995.**

Ref. 8 **W. J. O'Donnel and B, F, Langer, "Fatigue Design Basis for Zircaloy Components", Nucl. Sci. Eng. 20, 1, 1964.**

Ref. 9 **Regulatory Guide 1.77, "Assumptions used for evaluating a control rod ejection accident for Pressurized Water Reactors", NRC.**

Ref. 10 **R. Meyer, NRC, private communication, 1999.**

Ref. 11 **Dieter, G. E. Mechanical Metallurgy, McGraw-Hill Book Company, Inc., 1961**

Ref. 12 **Coffin, L. F."Localized Ductility Method for Evaluating Zircaloy-2 Cladding", Zirconium in the Nuclear Industry (Fourth Conference), ASTM STP 681, Am. Soc. for Testing and Materials, 72-87, 1979**

Ref. 13 **Dowling, N. E., Mechanical Behaviour of Materials, 2nd Edition, Prentice Hall, ISBN-0-13-905720-X, 1999**

Ref. 14 **Guy, A. G., Elements of Physical Metallurgy, 2nd EditionAddison-Wesley Publishing Company, Inc.**

Ref. 15 **Weertman, J.; Weertman, J. E.Elementary Dislocation Theory The Macmillan Company**

Ref. 16 **Franklin, D. G.; Lucas, G. E.; Bement, A. L.Creep of Zirconium Alloys in Nuclear Reactors, ASTM PCN 04-815000-35, ASTM, Philadelphia, 1983**

Ref. 17 **Lewis, J. E.; Schoenberger, G. ; Adamson, R. B. "Texture Measurement Techniques for Zircaloy Cladding: A Round-Robin Study", Zirconium in the Nuclear Industry: Fifth Conference, ASTM STP 754. D. G. Franklin Ed. Am. Soc. for Testing and Materials, 39-62, 1982**

Ref. 18 **Schemel, J. H, Zirconium Alloy Fuel Clad Tubing, Engineering Guide, 1st Edition, Sandvik Special Metals Corporation, December 1989**

Ref. 19 **Tenckhoff, E. Deformation Mechanisms, Texture, and Anisotropy in Zirconium and Zircaloy Special Technical Publication (STP 966), ASTM, 1988**

Ref. 20 **Rudling, P. and Adamson, R. B. "Zirat Special Topical Report on Manufacturing", ZIRAT, 2000**

Ref. 21 **Fidleris, V.; Tucker, R. P.; Adamson, R. B. "An Overview of Microstructural and Experimental Factors That Affect the Irradiation Growth Behavior of Zirconium Alloys," Zirconium in the Nuclear Industry, Seventh Int'l Symposium, ASTM STP 939, R. B. Adamson and L. F. P. Van Swam Eds., Am. Society for Testing and Materials, Philadelphia, 49-85, 1987**

Ref. 22 **Chalmers, B., Physical Metallurgy, John Wiley & Sons, Inc. 1962**

Ref. 23 **Van Bueren, H. G. Imperfections in Crystals, 2nd Edition North-Holland Publishing Company – Amsterdam, 1961**

Ref. 24 **Shishov, V. N., et al., "Influence of Zirconium Alloy Chemical Composition on Microstructure Formation and Irradiation Induced Growth", Zirconium in the Nuclear Industry – 13th Int'l Symposium, ASTM-STP XXXX, ASTM, to be published 2002**

Ref. 25 **Adamson, R. B., "Effects of Neutron Irradiation on Microstructure and Properties of Zircaloy", Zirconium in the Nuclear Industry: 12th Int'l Symposium, ASTM STP 1354, G. P. Sabol and G. D. Moan, Eds., Am. Soc. For Testing and Materials, West Conshohocken, PA, 15-31, 2000**

Ref. 26 **Rowland, T. et al., "Power Cycling Operation Tests of Zr-Barrier Fuel", Proc. Int'l Topical Meeting on LWR Fuel Performance. Fuel for the 90's, Avignon, France, 1991, 808-817**

Ref. 27 **Coffin, L. F., "Low Cycle Fatigue – A Thirty Year Perspective", GE CRD Report No. 84CRD236, 1984**

Ref. 28 **Dowling, N. E. Mechanical Behavior of Materials, 2nd Edition, Prentice Hall, 1999**

Ref. 29 **Dieter, G. E., Jr., Mechanical Metallurgy, McGraw-Hill Book Co., Inc., 1961**

Ref. 30 **Ransom, J. T., ASTM STP 121, ASTM, 59-63, 1952**

Ref. 31 **Grover, H. J., Fatigue of Aircraft Structures NAVAIR 01-1A-13, Naval Air Systems Command, Dept. of Navy, Washington, DC, 1966**

Ref. 32 **Sinclair, G. M.; Dolan, T. J. "Effect of Stress Amplitude on Statistical Variability in Fatigue Life of 75S-T6 Al-Alloy", Trans. Am. Soc. Of Mechanical Engineers, 867-872, 1953**

Ref. 33 **Richards, C. W. Engineering Materials Science, Wadsworth, Belmont, CA, 1961**

Ref. 34 **Hartmann, E. C.; Howell, F. M., "Laboratory Fatigue Testing of Materials", Metal Fatigue G. Sines and J. L. Waisman, Eds., Mc-Graw-Hill, New York, NY, 89-111, 1959**

Ref. 35 **Nakatsuka, M.; Kubo, T.; Hayashi, Y., "Fatigue Behavior of Neutron Irradiated Zircaloy-2 Fuel Cladding Tubes" Zirconium in the Nuclear Industry: Ninth Int'l Symposium, ASTM STP 1132, C. M. Eucken and A. M. Garde, Eds., Am. Soc. for Testing and Materials, 230-245, 1991**

Ref. 36 **Wisner, S. B.; Reynolds, M. B.; Adamson, R. B., "Fatigue Behavior of Irradiated and Unirradiated Zircaloy and Zirconium", Zirconium in the Nuclear Industry: Tenth Int'l Symposium, ASTM STP 1245, A. M. Garde and E. R. Bradley, Eds., Am. Soc. for Testing and Materials, Philadelphia, 499-520, 1994**

Ref. 37 **Armas, A. F.; Alvarez-Armas, I. "Cyclic Behavior or Zircaloy-4 at Elevated Temperatures", Zirconium in the Nuclear Industry: Seventh Int'l Symposium, ASTM STP 939, R. B. Adamson and L. F. P. Van Swam, Eds., Am. Soc. for Testing and Materials, Philadelphia, 617-630, 1987**

Ref. 38 **Kuto, T.; Motomiya, T.; Wakashima, Y. "Low-Cycle Corrosion Fatigue of Zircaloy-2 in Iodine Atmospheres" Journal of Nuclear Materials 140, North-Holland, Amsterdam, 185-196, 1986**